Public

Report

Document ID	Version	Status	Reg no	Page
1175236	2.0	Approved		1 (69)
Author U Ronneteg, L Cederqvist, T Öberg, C Müller			Date 2009-10-30	
Reviewed by			Reviewed date	
Approved by Håkan Rydén			Approved date 2011-03-04	

Reliability in friction stir welding of canister

Preface

This report is an updated version of the SKB report R-06-26, Reliability in sealing of canister for spent nuclear fuel, and have been produced by SKB (Ulf Ronneteg and Lars Cederqvist) together with our partners Tomas Öberg Konsult AB (Tomas Öberg) and Federal Institute for Materials Research and Testing, Berlin (Christina Müller).

The main changes in this report compared to the previous is that complementary data have been used for verification of the welding process and that a higher number of welds have been considered to cover the 6000 canisters (with both base and seal welds) according to the Swedish nuclear fuel programme.

Ver	Date	Description	Author	Reviewed	Approved
1.0	2009-02-27	New report	U Ronneteg L Cederqvist T Öberg C Müller	According SKBDoc id nr 1191972 ver 2.0	2009-06-25
1.4	2009-10-30 2011-02-28	Chapter 8 versionnumber for references added. Editorial corrections, after quality review. Unpublished references 10,11,25 deleated. Reference 14 changed to SIS 2000b. Referencelist changed to follow instruction 1215757.	U Ronneteg L Cederqvist T Öberg C Müller	Editorial corrections, no new fact review required	See head of page

Svensk Kärnbränslehantering AB
Swedish Nuclear Fuel and Waste Management Co
PO Box 925, S-572 29 Oskarshamn
Visiting address Gröndalsgatan 15
Phone +46-491-76 79 00 Fax +46-491-76 79 30
www.skb.se
556175-2014 Seat Stockholm

Summary

The reliability of the system for welding the canister and inspecting the weld that has been developed for the Encapsulation plant was investigated. In the investigation the occurrence of defects that can be formed in the welds was determined both qualitatively and quantitatively. The probability that these defects can be detected by non-destructive testing (NDT) was also studied.

The friction stir welding (FSW) process was verified in several steps. The variables in the welding process that determine weld quality were identified during the development work. In order to establish the limits within which they can be allowed to vary, a screening experiment was performed where the different process settings were tested according to a given design. In the next step the optimal process setting was determined by means of a response surface experiment, whereby the sensitivity of the process to different variable changes was studied. Based on the optimal process setting, the process window was defined, i.e. the limits within which the welding variables must lie in order for the process to produce the desired result. Finally, the process was evaluated during a demonstration series of 20 welding welds which were carried out under production-like conditions. To further verify the robustness of this study an additional welding series (post demonstration), of 20 short welds, with optimized tool geometry were performed.

Conditions for the formation of defects in welding were investigated. The investigations show that the occurrence of defects is dependent on the welding variables. Defects that can arise were classified and described with respect to characteristics, occurrence, cause and preventive measures.

To ensure that testing of the welds has been done with sufficient reliability, the probability of detection (POD) of defects by NDT and the accuracy of size determination by NDT were determined.

In the evaluation of the demonstration series, a statistical method based on the generalized extreme value distribution, was fitted to the size estimate of the indications obtained with NDT. The predicted maximum defect size in connection with the welding of 6,000 canisters with the present process development was conservatively determined to be less than one centimetre. All factors considered, the predicted minimum copper coverage for a 5 cm thick canister is 4 cm.

Acceptance criteria for permitted settings in the welding process in a future welding system are proposed, as is the use of statistical process control based on non-destructive testing as an independent inspection system. Furthermore, principles for handling of process non-conformances are presented.

Contents

1 Background

This report comprises a basis for SKB's safety assessment SR-Site. SR-Site analyzes the long-term safety of a KBS-3 type final repository, where copper canisters with a cast iron insert are filled with spent nuclear fuel and deposited at a depth of approximately 500 metres in granitic rock surrounded by bentonite clay. SR-Site is based on site data from SKB's ongoing investigations of candidate sites for a final repository for spent nuclear fuel in Forsmark and Laxemar. SR-Site will comprise a basis for SKB's application for a permit to build a final repository and an encapsulation plant. The canister's initial copper coverage is a crucial item of information for the assessments of the long-term safety of the repository, and the quality of the canister's welded joints, which is the subject of this report, is a cornerstone of this issue.

The strategy that has been applied to obtain data for the assessment of the long-term safety of the final repository entails determination of the reliability of the processes included in the future production system. The production system is divided into three sections:

- Copper section, used to produce the copper shell and includes fabrication and inspection of copper components for canisters that are delivered to the encapsulation plant.
- Insert Section, used to produce the cast iron insert and includes fabrication and inspection of the insert and its components.
- Weld Section, used to seal the copper shell and includes welding (base and lid weld), machining and inspection of the welds.

This report concerns the reliability of the Weld Section. Similar investigations for the Copper and Insert sections are described in the reliability reports for the actual sections.

The first theoretical discussions of the programme for reliability in welding and NDT processes were presented in the planning report SR-Can /SKB, 2003/. The final strategy and the methods intended to be used were presented in 2004 /Müller and Öberg, 2004/. In 2006 SKB presented the first analysis /Ronneteg U, et al, 2006/ of the reliability of the sealing process and this report covers mainly this analysis completed with additional experiments. The timetable for the programme was presented in SKB's RD&D-programme /SKB, 2004/. The main points in the programme have been:

1) Verification and demonstration of the welding processes electron beam welding (EBW) and friction stir welding (FSW).
   - Investigation of the robustness of the processes with respect to permissible variations in the process variables.
   - Verification that the processes can be carried out on full scale by welding of a complete canister.
   - Demonstration of serial production capacity and achieved weld quality by welding 20 lids for each welding process.
2) Investigation of reliability in non-destructive testing (NDT) of the welding process.
3) Statistical analysis and prediction of future production quality.

Up until March 2005, SKB worked in parallel on the development of two welding methods at the Canister Laboratory: friction stir welding (FSW) and electron beam welding (EBW). For the continued work leading up to a permit application for the encapsulation plant, May 2005 was deemed to be a suitable time to choose a reference method for welding. The criteria for choice of reference method are described in greater detail in /SKB, 2006a/. Now that FSW has been chosen as the reference method, the in-depth analysis work has been concentrated on FSW and the results are only reported for FSW.

2 Purpose of the report

The purpose of the report is to give an account of:

- The reliability of the welding process.
- The reliability of the NDT process developed in parallel with the welding process.
- The predicted reliability of the welding section, including both welding and NDT processes in the future production.
- The programme for verification and demonstration of the welding process that was mentioned in SKB's RD&D-programme /SKB, 2004/.

The outline of the report is as follows:

Chapter 3. Description of the FSW system at the Canister Laboratory and the welding process that has been developed.

Chapter 4. Account of how verification of the welding method has been done. The chapter describes the investigations of the various process settings, how they interact and the size of the process window.

Chapter 5. Description of the processes and systems for NDT that have been developed to detect defects in the weld metal.

Chapter 6. Account of defects that can occur in welds made by FSW.

Chapter 7. Account of the reliability of the NDT processes.

Chapter 8. Description of the demonstration series and the post-demonstration series. An account is given of operating experience and the quality of the welds.

Chapter 9. Prediction of the future production quality of welding of 6000 canisters.

Chapter 10. Presentation of proposed acceptance criteria for Weld Section.

Chapter 11. Conclusions.

Chapter 12. Future line of action.

Chapter 13. References.

Chapter 14. Abbreviations.

3 Friction stir welding (FSW)

Friction stir welding (FSW) is a type of friction welding that was invented in 1991 at The Welding Institute in Cambridge, England. FSW is a thermo mechanical solid-state process, i.e. not a fusion welding method. This means that the problems encountered in fusion welding – such as unfavourable grain structure, grain growth and segregation phenomena – can be avoided. The resulting microstructure in FSW of copper thus resembles the microstructure resulting from hot forming of the copper components in the canister. The process and system are described in this chapter.

3.1 Description of the welding process

A rotating welding tool consisting of a tapered probe and shoulder, see Figure 3-1, are plunged into the weld metal. The function of the probe is to heat up the weld metal by means of friction and, by virtue of its shape and rotation, force the metal to flow around it and create a weld. The function of the shoulder is to heat up the metal by means of friction and prevent it from being squeezed out of the joint. Figure 3-2 shows when the tool is advanced along the joint and forms a weld.

Figure 3-1. *The welding tool.*

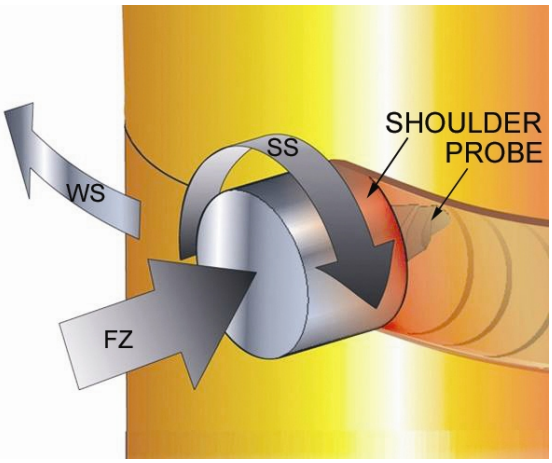

Figure 3-2. *S Schematic diagram of the friction stir welding process and the important welding factors (SS=tool rotation speed, WS=welding speed, and FZ=axial force).*

One reason for the rapidly increasing use of FSW in industry is that the method has few welding variables. This means that the welding process is simple to control. The welding tool rotates at a specific number of revolutions per minute and moves along the joint at a constant speed. The position of the tool shoulder in relation to the canister surface is then controlled with a specific downward force. In most cases the tool is also angled in relation to the work-piece so that the tool shoulder “surfs” on the surface.

Besides the adjustable variables (called welding factors), the resulting variables (called welding responses) are measured. These factors are the depth of the shoulder in the weld metal, the tool temperature, the torque of the spindle motor and the force on the tool in the direction of travel.

There is a clear relationship between welding factors and welding responses, for example the product of the rotation speed and the torque of the spindle motor are equal to the heat input and thereby affect the temperature of the tool. These relatively elementary relationships make the process simple to interpret, develop and control.

The welding machine that is used in the Canister Laboratory has cooling of both the lid clamps and the tool holder. However the cooling has a secondary influence on the process. The purpose of cooling is to protect the machine against high temperatures and reduce wear on the spindle motor and the tool holder.

A weld cycle can be divided into several sequences, which are shown in Figure 3-3. First a start hole is drilled 75 mm above the joint line which the rotating tool is then plunged into so that the copper is heated. When the tool temperature has reached a set value, the welding speed is accelerated to a constant value. After the acceleration sequence is finished and the tool temperature has stabilized, i.e. reached the "steady-state" value, the tool is moved down to the joint line. After a full revolution (360º) at the joint line, the tool is moved up 75 mm above the joint line, where the welding cycle is terminated and the tool is withdrawn resulting in the unavoidable exit hole. Both the acceleration sequence and the exit hole are then machined off when the lid is given its final dimensions.

The acceleration sequence is important since it affects flash formation and the risk of defects during the downward sequence. The other sequences, nos. 2-5 in Figure 3-3, can be merged into the "steady-state" sequence where all variables remain at a relatively constant value.

After the canister is positioned in the machine, it takes about an hour to seal the canister, including clamping of canister and lid (5 minutes), drilling of start hole (5 minutes) and welding (50 minutes). The time required for the process in the encapsulation plant is estimated to be equivalent. Experience from the Canister Laboratory shows that the capacity is sufficient and that several canisters can be sealed each day.

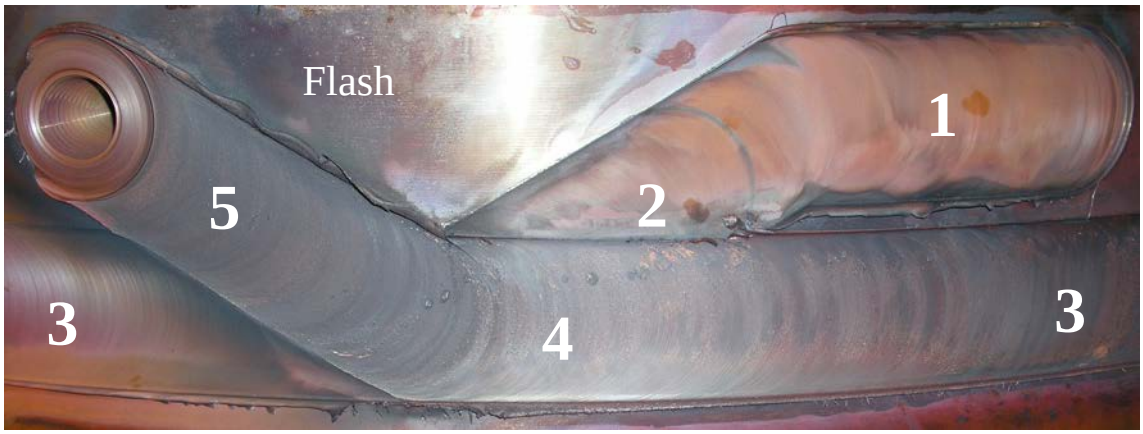

Figure 3-3. *Sequences in a weld cycle: 1. acceleration sequence, 2. downward sequence, 3. joint line sequence, 4. overlap sequence, and 5. parking sequence.*

3.2 Description of the welding system

In early 2002 a welding machine designed for full-scale welding was ordered from ESAB AB in Laxå, see Figure 3-4.

Prior to welding the canister is raised into the welding machine by the canister manipulator. When the canister has been positioned in the machine, it is clamped in expanding pressure jaws, see Figure 3-5. The total pressure amounts to 3200 kN, distributed among 12 jaws. In the next step the lid clamps are expanded, see Figure 3-6, and a pressure of 390 kN presses the lid down against the canister. A start hole is drilled, see Figure 3-7, with a separate drill unit next to the spindle and the weld cycle is started by plunging the rotating tool into the hole, see Figure 3-8. During the process the welding heat rotates around the canister. The maximum angle of rotation is 425 degrees.

Figure 3-4. The welding machine at the Canister Laboratory.

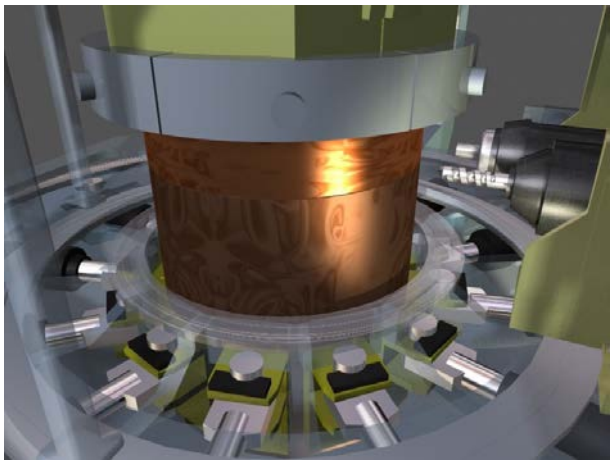

Figure 3-5. *Clamping of copper canister.*

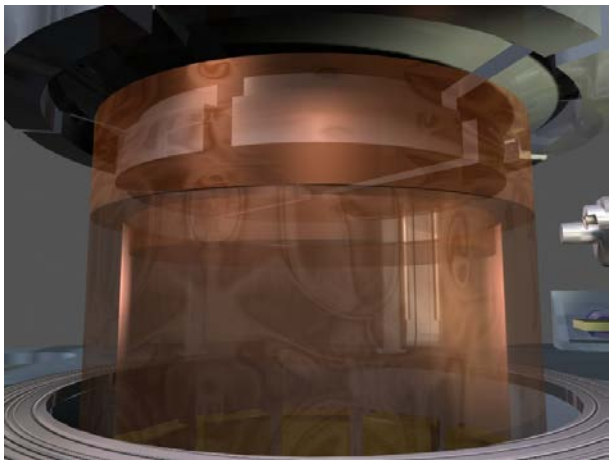

Figure 3-6. *Clamping of lid.*

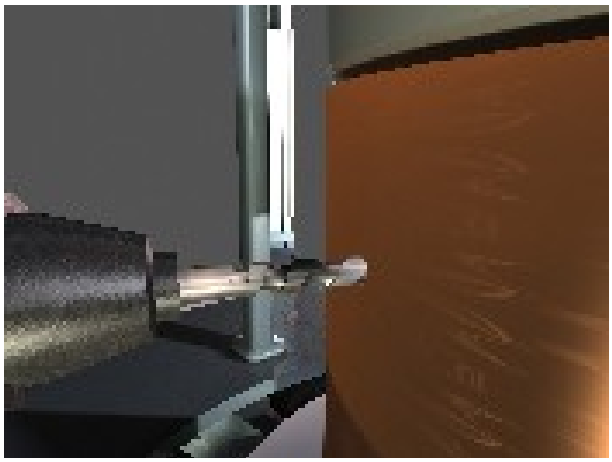

Figure 3-7. Drilling of start hole.

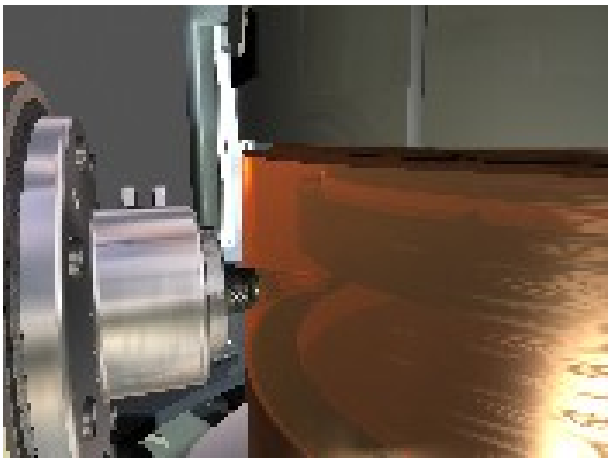

Figure 3-8. Tool in start hole.

The tool (see Figure 3-1) is an important component in FSW. The tool must withstand a high process temperature, as well as the high forces to which it is subjected during welding. A weld takes about 50 minutes and is four metres long.

A nickel-base superalloy (Nimonic 105) is used as the material in the tool probe. Nickel-base alloys have good high-temperature properties with good wear resistance and sufficient strength for canister welding. The tool shoulder is made of a tungsten alloy (Denismet) with suitable thermal and mechanical properties for the process. The probe is changed after each weld while the shoulder can be used for several welds.

The software that monitors the welding process logs all variables every tenth of a second, i.e. with a frequency of 10 Hz. During the welding process, selected variables are displayed numerically and graphically to the welding operator. Two video cameras also show the tool from the rear and the front. All regulation of the welding process is currently performed manually by the welding operator (at present by changes in spindle speed and/or axial force). As described in the future line of action in Chapter 12, the development of a fully automated welding process is an important milestone prior to qualification of the welding system and welding procedure.

Since the tool temperature has proved to be very important, two separate and independent measurements of this variable are currently made. Since the installation of the welding system, a thermocouple has been placed in the tool probe to measure the temperature during the weld cycle, which is the value reported as the tool temperature in this report. An infrared camera was also installed in the autumn of 2005 to measure the temperature of the tool shoulder. This has proved to be an excellent complement to the thermocouple in the tool /SKBdoc 1175162/.

4 Verification of the welding process

The FSW process was evaluated by means of a statistical methodology (see Figure 4-1) aimed at optimizing process settings and determining the process window /Müller and Öberg, 2004; Box and Draper, 1987; Box et al, 1978/. In order to verify the welding process, the welding variables that determine weld quality were identified. Then the limits within which these variables (welding factors) could be allowed to vary were determined by a screening experiment. In the next step a so-called response surface experiment was conducted to determine the optimal process setting and then the process window was defined. Finally, the optimized process was evaluated by demonstration series under production-like conditions which are covered in chapter 8.
Results from this reliability study have also been reported in a scientific peer-reviewed journal /Cederqvist and Öberg, 2008/.

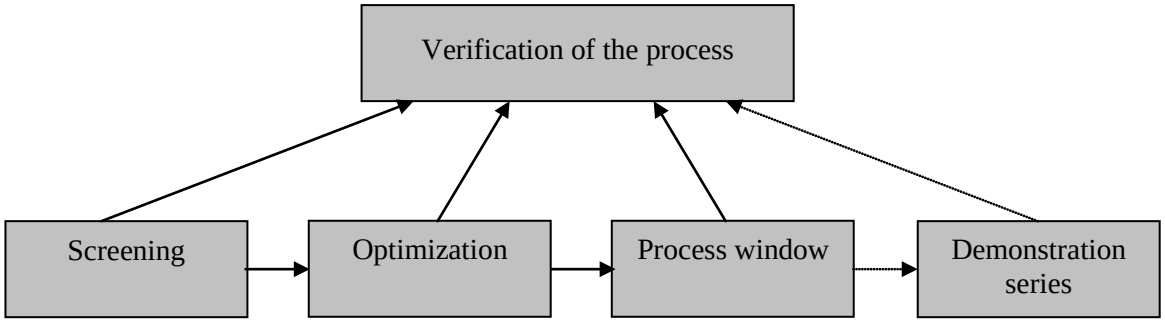

Figure 4-1. *Verification of the welding process.*

4.1 Screening

As described previously in section 3.1, there are four welding factors that can be varied and four welding responses that are monitored. Experience from previous welding trials, shows that the welding responses that are most important for the weld quality are the depth of the shoulder in the canister and the temperature of the tool. Suitable values, based on early welding trials, for shoulder depth and tool temperature are 0.6 mm and 855 °C.

The desired value for tool temperature applies during the joint line sequence, while the desired value for shoulder depth only applies during the acceleration sequence, the downward sequence and approximately ten degrees of joint line welding. After these sequences, this variable cannot be used to control the process since it is not possible to obtain an accurate value of the shoulder depth. The reason for this is a combination of the fact that the canister is not perfectly centred in the welding system, deflections in the welding system and thermal expansion of the canister.

The screening experiments comprise three lid welds consisting of 22 separate weld cycles. A wide range of values was tried for each welding factor (Table 4-1) and the effect of this variation on the welding responses (Table 4-2) was studied /Cederqvist, 2006/.

Table 4-1. Welding factors, screening experiments.

Variable	Unit	Tested range
Welding speed (WS)	mm/min	60-130
Spindle speed (SS)	rpm	350-500
Axial force (FZ)	kN	70-105
Tool angle	°	2-4

Table 4-2. Welding, screening experiments. responses.

Variable	Unit	Tested range
Shoulder depth	mm	0-4
Tool temp.	°C	690-945
Spindle torque	Nm	750-1200
Traverse force	kN	25-70

The screening experiments showed that the tool angle did not notably affect the weld quality within the tested range. As a result, spindle speed, welding speed and axial force were chosen in the optimization study.

4.2 Optimization

The response surface method was used to optimize the process. Three welding factors were varied in the trial series: welding speed (WS), spindle speed (SS) and axial force (FZ). The choice of variation range is shown in Table 4-3. Low, medium and high level for each factor is indicated by -1, 0 and 1, and represents a cold, medium and hot parameter setting respectively.

Table 4-3. Levels for the different welding factors in the response surface experiment.

Level / factor	-1	0	1
WS: (mm/min)	100	80	60
SS: (rpm)	360	400	440
FZ: (kN)	86	89	92

Each test entailed welding for 45 degrees, permitting eight tests along the lid circumference. The number of tests in the trial series was 16, and they were performed on two welding welds. The chosen experimental plan, a response surface experiment according to Box-Behnken, permits estimation of an empirical polynomial model with linear interaction and quadratic terms /Box and Draper 1987/. The experimental plan is shown in Table 4-4. The response surface models (polynomial) were fitted to the measurement data by multiple linear regression. The model terms (interactions) that were not significant were removed, and the final models contained three linear and three quadratic terms.

Table 4-4. Experimental plan for response surface experiment.

Test	Weld	Segment	Welding speed (WS)	Spindle speed (SS)	Welding force (FZ)
1	1	0-45°	0	0	0
2	1	45-90°	1	0	-1
3	1	90-135°	0	-1	1
4	1	135-180°	0	0	0
5	1	180-225°	1	0	1
6	1	225-270°	-1	0	1
7	1	270-315°	0	0	0
8	1	315-360°	0	-1	-1
9	2	0-45°	-1	-1	0
10	2	45-90°	0	1	-1
11	2	90-135°	1	-1	0
12	2	135-180°	-1	1	0
13	2	180-225°	0	1	1
14	2	225-270°	0	0	0
15	2	270-315°	-1	0	-1
16	2	315-360°	1	1	0

The values of the shoulder depth and the tool temperature at the end of each test (see Table 4-5) were used to evaluate the experiments and choose optimal settings for further operation. The desired values for shoulder depth and tool temperature were 0.6 mm and 855 °C, respectively. Since the tests were at most 45 degrees, the value of the shoulder depth is considered accurate since the centring and thermal expansion of the canister only affected the value marginally.

Table 4-5. Results of response surface experiment.

Test	Shoulder depth (mm)	Tool temperature (°C)
1	1.0	820
2	0.8	885
3**	0.4	750
4**	1.0	760
5**	1.6	920
6**	0.9	760
7	0.5	790
8	0.4	770
9**	0.8	770
10**	2.2	910
11	1.1	820
12**	2.8	920
13**	2.4	930
14*/**	(2.4)	(880)
15	0.5	730
16**	2.2	920

* = Test 14 was excluded because a poor start hole may have affected the result.
**= To avoid the risk of damaging the welding system, these tests were terminated before 45 degrees was reached.

The two regression models that were fitted to these data were both statistically significant. The variance contribution from each welding factor is shown in Tables 4-6 and 4-7[1].

Table 4-6. Analysis of variance for a response surface model with regard to shoulder depth.

Source		s.s.	d.f.	m.s.	F	P
Model		8.08	6	1.35	13.19	0.0009
	WS	0.061	1	0.061	0.60	0.4609
	SS	5.95	1	5.95	58.30	<0.0001
	FZ	0.24	1	0.24	2.40	0.1599
	WS^2	0.22	1	0.22	2.19	0.1775
	SS^2	1.54	1	1.54	15.09	0.0046
	FZ^2	0.062	1	0.062	0.60	0.4596
Residuals		0.82	8	0.10		
	Model error	0.65	6	0.11	1.30	0.4958
	Experimental error	0.17	2	0.083		
Total		8.90	14			

[1] Acronyms in the analysis of variance tables: s.s. = sum of squares, d.f. = degrees of freedom, m.s. = mean squares (s.s./d.f.), F = test quantity (ratio of ss for model to residuals, or model error to experimental error) and P = probability in relation to the F distribution.

Table 4-7. Analysis of variance for a response surface model with regard to tool temperature.

Source		s.s.	d.f.	m.s.	F	P
Model		66173	6	11029	6.92	0.0078
	WS	16653	1	16653	10.45	0.0120
	SS	40612	1	40612	25.48	0.0010
	FZ	528.1	1	528.1	0.33	0.5807
	WS^2	2424	1	2425	1.52	0.2524
	SS^2	6474.	1	6475	4.06	0.0786
	FZ^2	243.8	1	243.8	0.15	0.7059
Residuals		12750	8	1594		
	Model error	10950	6	1825	2.03	0.3666
	Experimental error	1800	2	900.0		
Total		78923	14			

The importance of the different welding factors within the investigated domain is shown directly by the P values. Welding speed (WS) only influences tool temperature, while spindle speed (SS) is important in both cases. The evaluation can also be done by examining the disturbance plots, where the effect of changing one welding factor at a time is shown, see Figures 4-2 and 4-3. The effects can be examined independently of each other, since there is no interaction in the investigated process window.

The agreement between model predictions and measurement results is shown in Figures 4-4 and 4-5.

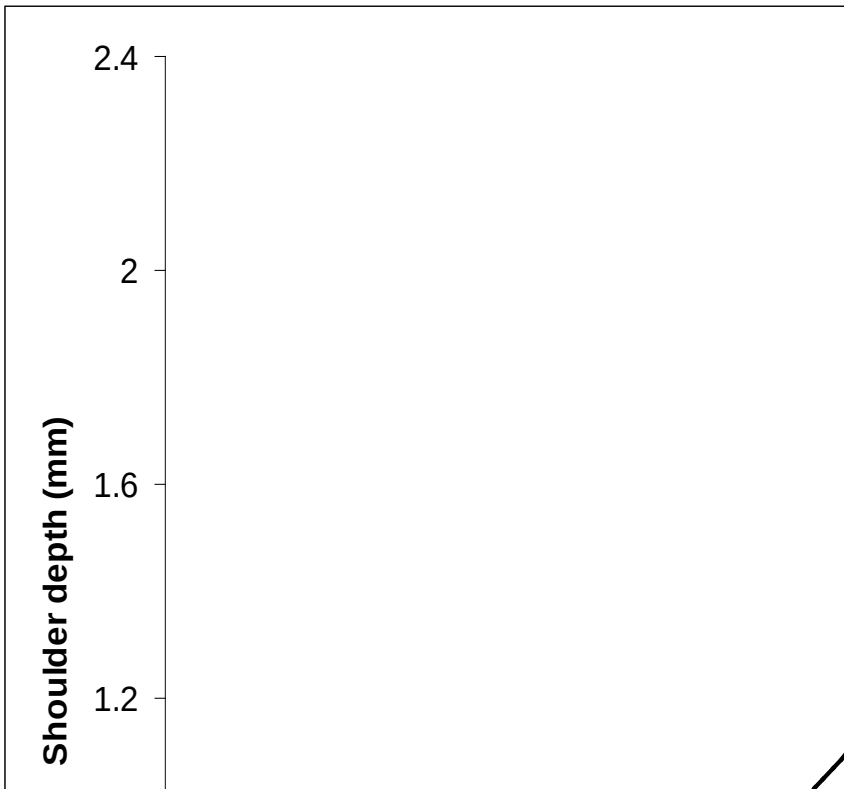

Figure 4-2. *Influence on shoulder depth between high and low level for the relevant welding factor.*

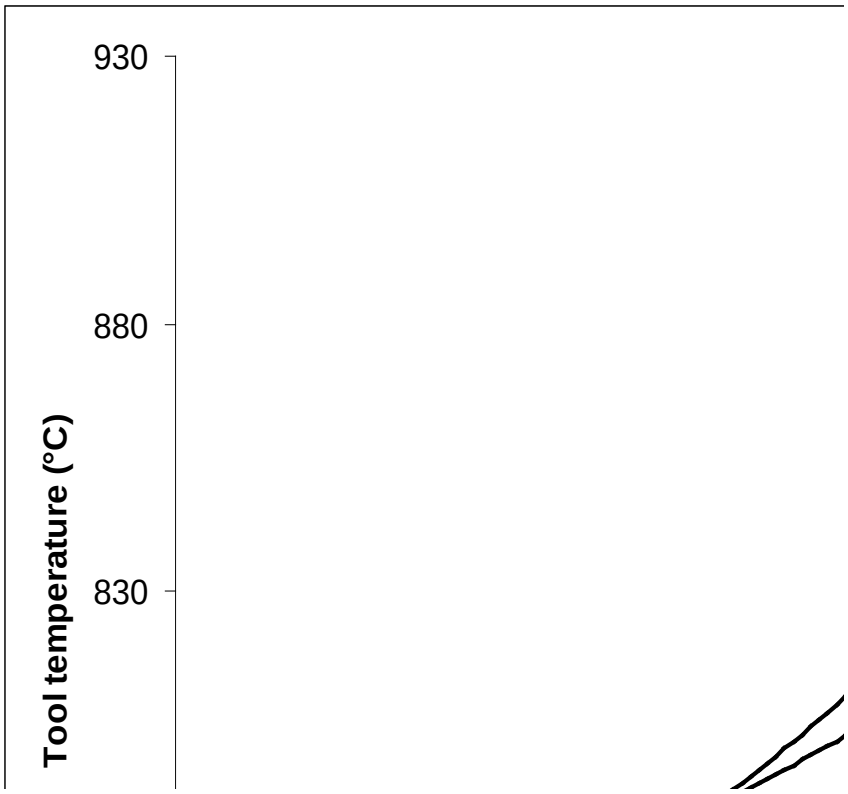

Figure 4-3*. Influence on tool temperature between high and low level for the relevant welding factor.*

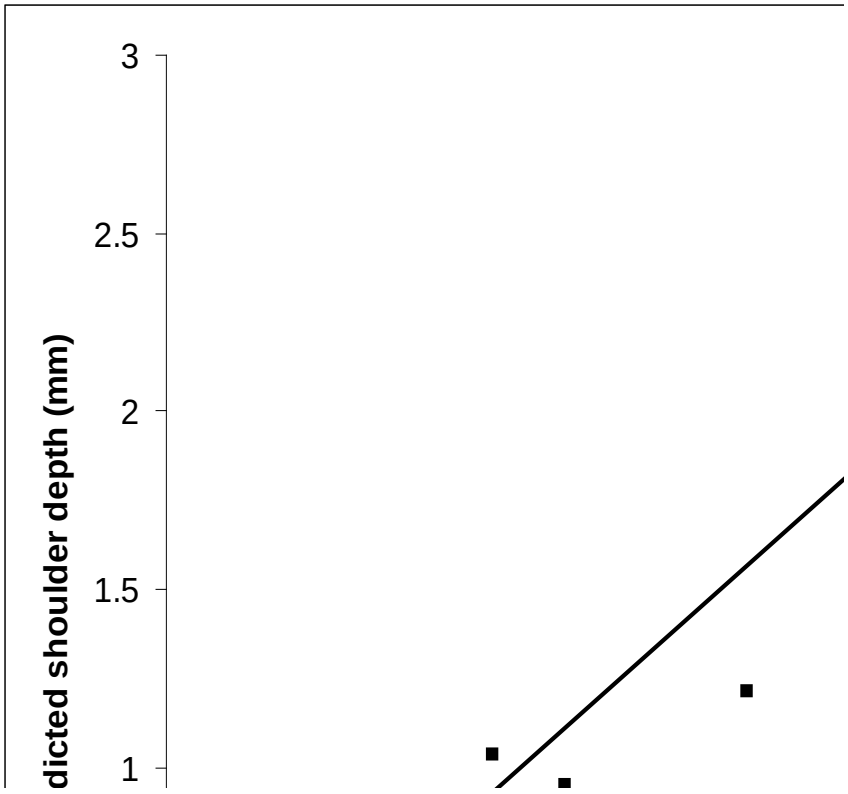

Figure 4-4. *Predicted vs. measured shoulder depth (mm).*

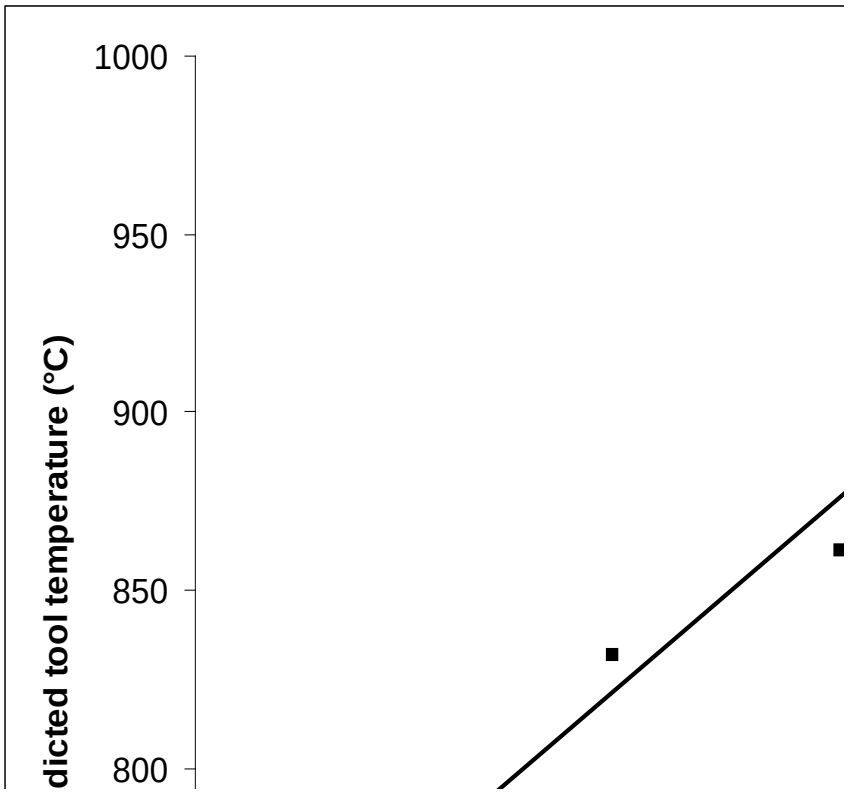

Figure 4-5. *Predicted vs. measured tool temperature (°C).*

The conclusions of the response surface experiment are:

- In the early welding trials, weld quality and the welding responses were controlled by means of small changes (0.5 kN) in axial force. However, the response surface experiment shows that spindle speed is the most important factor, which makes it more suitable for controlling the process.
- Welding speed was the next most important welding factor. Its influence on tool temperature was similar to that of spindle speed. This factor should, however, be kept constant to not increase the risk of forming defects.
- The variations in axial force were of no importance within the studied range, which meant that it should be used as a secondary control factor.

A suitable operating setting entails a compromise between the two optimization criteria (the previously called desired values for shoulder depth and tool temperature). Based on the response surface experiment, the optimal values for the welding factors were found to be: welding speed 74.3 mm/min, spindle speed 410 rpm and axial force 87 kN. According to the response surface models, this process setting will result in a shoulder depth of 0.96 (±0.36) mm and a tool temperature of 824 (±45) °C (standard errors within parentheses).

4.3 Process window

The process window is the permissible interval within which the welding factors and welding responses may vary from the optimal values established in the response surface experiment without the weld quality being affected.

In order to verify the modified control of the welding process (by means of the spindle speed) and determine the process window, welding trials on three lids were carried out. Table 4-8 shows the tested window at a welding speed of 74.3 mm/min. Control of the process by means of the spindle speed proved to be excellent with more effective and quicker response than when axial force was used.

The process windows for the welding factors, spindle speed and axial force, are the same as the tested interval, since no risk of defects could be demonstrated. In other words, these process windows are presumably much greater, which could be established in a more detailed study (see Chapter 14).

However, the process window for the welding responses, tool temperature and shoulder depth, is more strongly linked to weld quality. The correlations between the welding responses and the weld quality have been established from the screening and optimization tests, and the tests at a welding speed of 74.3 mm/min confirmed these correlations. At tool temperatures above 910°C there is a risk of tool failure /Cederqvist, 2006/, and below 790°C defects have been encountered. At a shoulder depth below 0.4 mm there is a risk of defects, and at a high value (above 1.5 mm) there is a risk that the welding process will be difficult to control with defects as a result. The process window for the welding responses is illustrated graphically in Figure 4-6 and contains the results from the response surface experiment at the end of the acceleration sequence plus the results from the response surface models for the chosen process setting.

As Table 4-8 shows, the tested process window for tool temperature is 790-910°C. To put this window in perspective it can be compared with welding factors and responses from the first lid weld after the demonstration series. Figure 4-7 shows welding factors and responses from the "steady-state" sequence, i.e. sequence 2-5 in Figure 3-3 in a weld, which is equivalent to a welding distance of 390 degrees or 45 minutes. The tool temperature lies between 835 and 860°C, i.e. ±12°C compared with the process window of ±60°C.

Table 4-8. Determined process window.

Factor/response	Window	At high value	At low value
Spindle speed (rpm)	350-450	Risk of high tool temperature	-
Axial force (kN)	78-98	Risk of high tool temperature	Risk of defects
Tool temperature (°C)	790-910	Risk of tool failure	Risk of defects
Shoulder depth (mm)	0.4-1.5	Risk of defects	Risk of defects

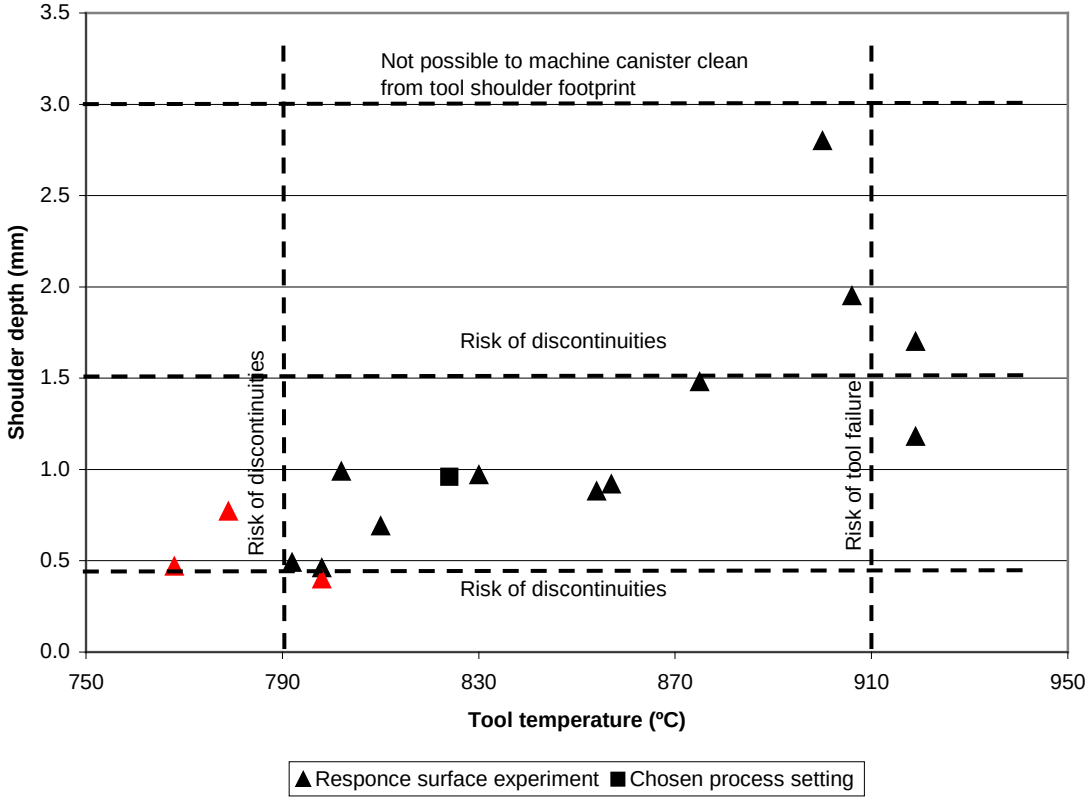

Figure 4-6. *Process window for welding responses including data from response surface experiment (red points refer to welds with defects).*

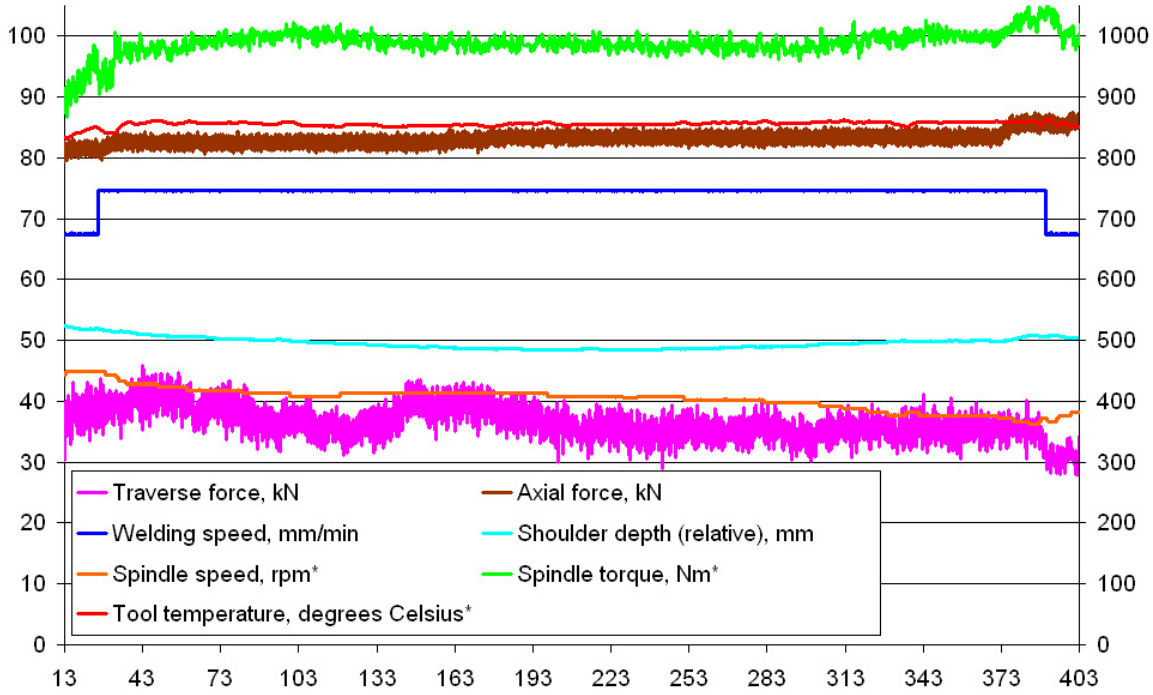

Figure 4-7. *Welding factors and responses from lid weld. * value on right-hand y axis.*

4.4 Alternative evaluation of response surface experiment

A number of tests in the response surface experiment did not reach steady-state, see Table 4-5, and had to be terminated before 45 degrees had been welded to not risk damage (due to high forces and/or high temperature) to the welding system. In order to verify that this did not affect the analysis, an alternative analysis was subsequently carried out on the welding tests in Table 4-4 . In this analysis, welding variables in an earlier stage of the weld cycle (at the start of the downward sequence) were used, since no tests had been terminated at that point. The values for shoulder depth and tool temperature at this important stage of the weld cycle are shown in Table 4-9.

The conclusions from the alternative analysis of the response surface experiment are:

- The two regression models that were fitted to these measurement data are statistically significant.
- The relationships between welding factors and welding responses are essentially similar to the original analysis with spindle speed as a suitable welding factor to control the process. However, these models exhibit a slightly poorer fit to the measurement data, especially the model for shoulder depth, which is however still statistically significant.
- The welding speed was found not to be a significant factor in the response surface model for tool temperature. This result is understandable, since it is an early stage of the weld cycle where welding speed has not had time to influence the process.
- The optimal values for the welding factors that were determined in Chapter 4.2 give a similar outcome, with a shoulder depth of 0.81 (±0.45) mm and a tool temperature of 833 (±32) °C, for the alternative response surface analysis (standard errors within parentheses). The similar results show that the original analysis was not markedly affected by the early terminated tests.

Table 4-9. Modified results of response surface experiment.

Test	Shoulder depth (mm)	Tool temperature (°C)
1	0.9	854
2	0.7	810
3	0.5	768
4	1.0	802
5	1.5	875
6	0.9	857
7	0.5	798
8	0.4	798
9	0.8	779
10	1.7	919
11	1.0	830
12	2.8	900
13	1.2	919
14*	(1.5)	(834)
15	0.5	792
16	1.9	906

* = Test 14 was excluded because a poor start hole may have affected the result.

5 Non-destructive testing (NDT)

This section describes the NDT processes that are used for testing of the welds. For a more comprehensive report on the work with non-destructive testing of the weld, see /SKBdoc 1179633/.

Welds with different purposes and therefore of varying quality have been produced during the welding development work, providing an opportunity for optimization of the testing methods. Altogether, more than 60 welds have been examined by radiographic and ultrasonic testing, most of these both before and after machining. Testing has been carried out according to written procedures to ensure traceability and consistent assessment.

5.1 Description of NDT systems

A radiographic and an ultrasonic system are used at the Canister Laboratory for NDT of the sealing and base welds.

5.1.1 System for phased array ultrasonic testing

In ultrasonic testing based on phased array technology, an ultrasound sensor with a large number of probe elements is used. The technology permits electronic focusing and control of the sound beam. The Canister Laboratory's system for phased array ultrasonic testing consists of the following main components (Figure 5-1):

- Manipulators for inspection of welds performed on both full-scale canisters as short copper rings.
- Fixtures for ultrasound transducers for calibration and inspection.
- Phased array ultrasound equipment and linear array probes.

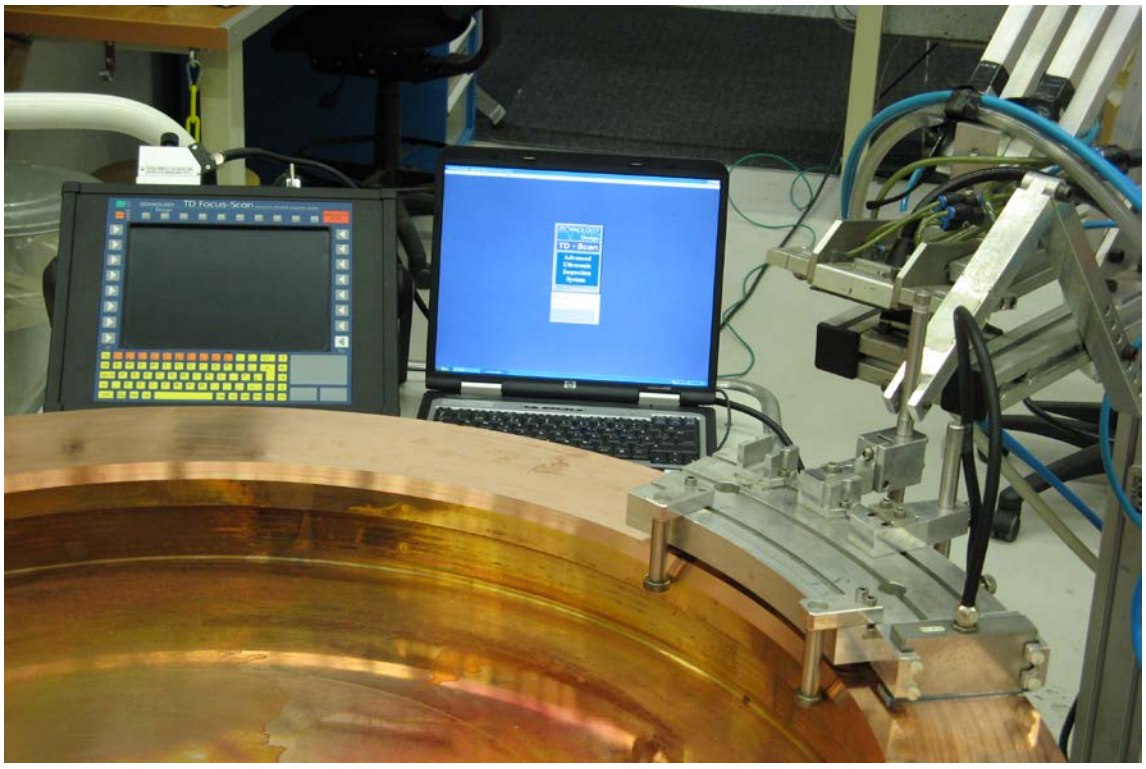

Figure 5-1. *Ultrasonic inspection unit for testing of the copper canister's sealing and base welds.*

5.1.2 System for digital radiography

The Canister Laboratory's system for digital radiography consists of the following main components (Figure 5-2):

- 9 MV linear accelerator.
- Detector system with a linear detector.
- Manipulator for positioning of accelerator and detector.
- Software for control of the process and evaluation of results.

The accelerator has exceptional performance when it comes to generating X-rays with high energy and a high dose rate. Due to the high dose rate of up to 3000 rad/min, the influence of a canister with spent nuclear fuel on the testing can be regarded as negligible, 0.2–2% (calculated based on the canister's surface dose rate /SKBdoc 1077122/). This value is calculated assuming that the canister's radiation has the same uniform direction as the X-rays. In reality, however, the direction of the radiation from the fuel is randomized, which means that this value is much lower.

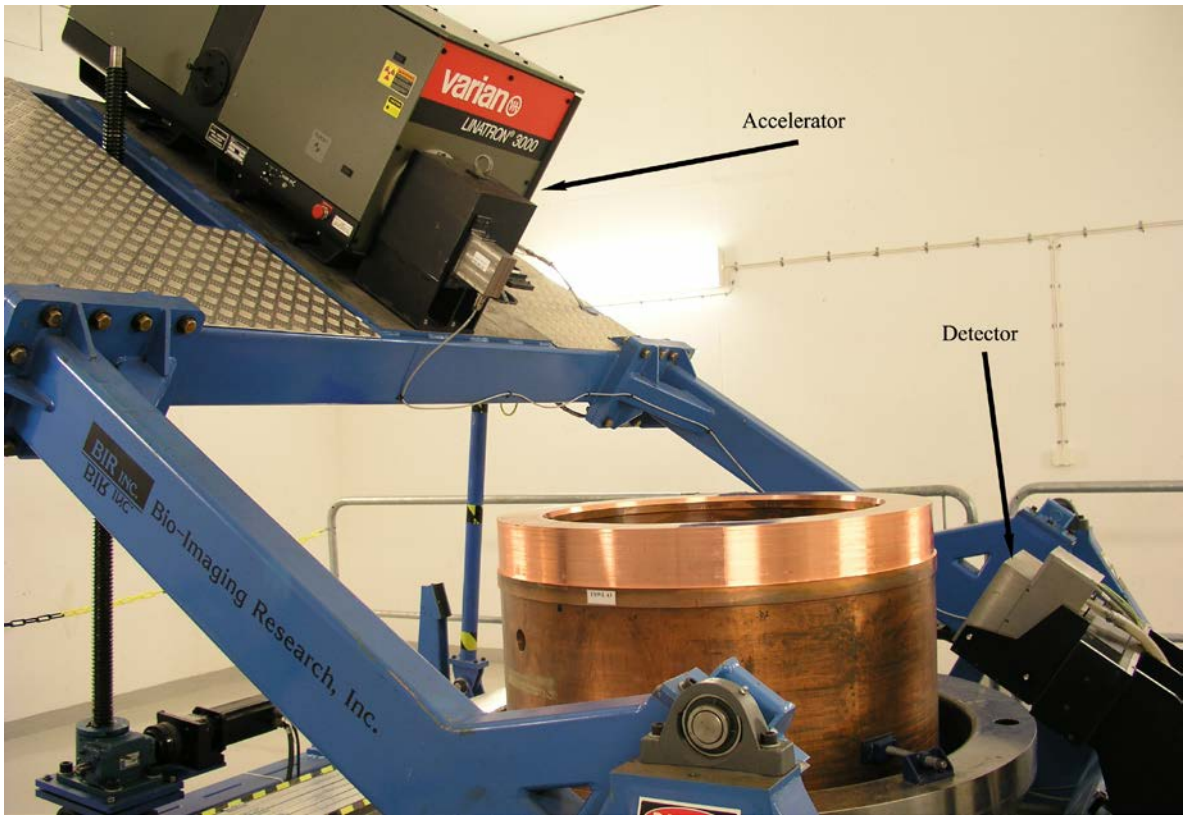

Figure 5-2. *X-ray machine for testing of the copper canister's sealing and base welds.*

5.2 Description of NDT processes

In order to ensure good and repeatable quality in non-destructive testing of the canister's lid weld, procedures have been established for testing and evaluation. They include software settings, mechanical settings, reference normals and evaluation criteria.

5.2.1 Principles of phased array ultrasonic testing

The testing principle is that the canisters rotates while an ultrasound probe, with 5 MHz centre frequency, electronically scans the sound beam in the radial direction (see Figure 5-3). In order to ensure coupling of the sound waves inside the canister, a thin water film is used as a coupling agent. To ensure that testing covers the whole weld with respect to possible defects (Chapter 6), the sound is focused electronically on different depths and with varying angles in the radial direction. The results are presented in the form of a two-dimensional image (C-scan), see Figure 5-4, composed of the maximal amplitude for each index point. The results are evaluated by locating indications with an amplitude above a given threshold value and determining their size by the half value method /SIS, 2000/.

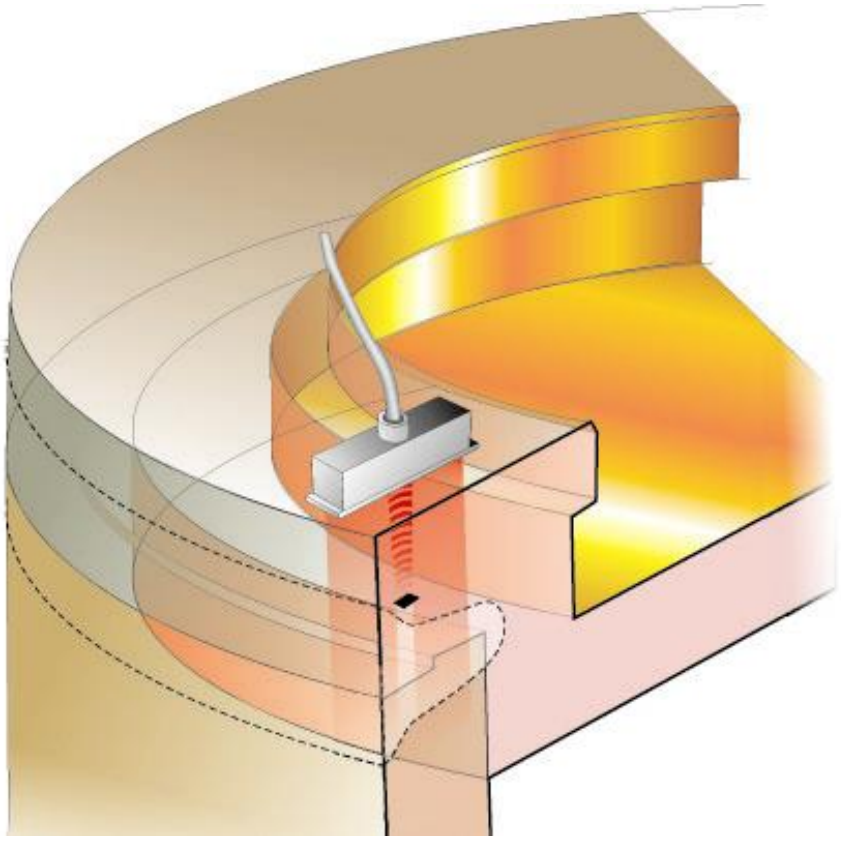

Figure 5-3. *Principle of ultrasonic testing of FSW.*

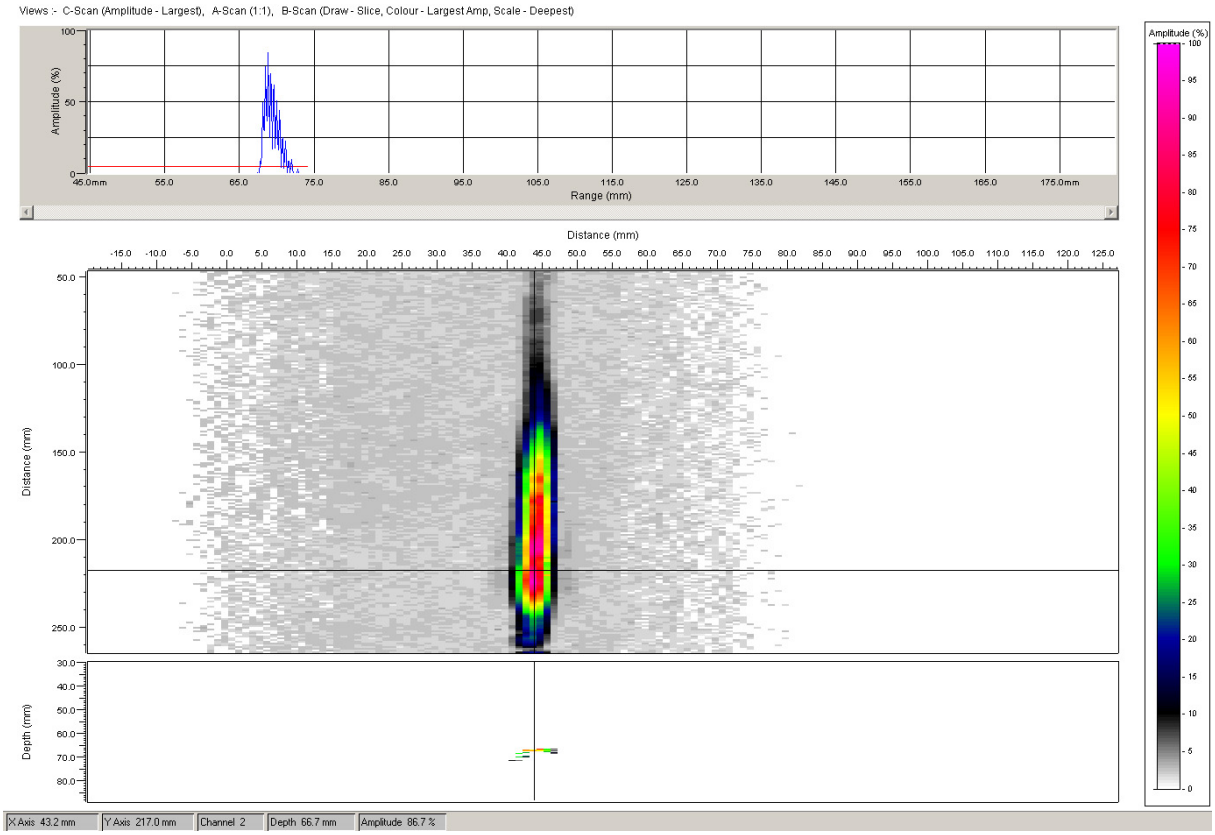

Figure 5-4. *Ultrasound of FSW, A-scan at top, C-scan in middle and B-scan at bottom.*

5.2.2 Principles of digital radiography

The main principle is that the canister rotates while the accelerator pulses X-rays through the weld with an incident angle of 35° (see Figure 5-5 below). The transmitted radiation is detected by a linear detector (100 mm high) positioned perpendicular to the beam with a vertical resolution (channel width) of 0.4 mm. This same resolution is achieved in the vertical direction by a collimator (vertical gap) that focuses the beam, and the X-ray image is built up with every 0.4 mm rotation of the canister (see Figure 5-6 below). The result is then evaluated using criteria based on the geometry of the canister in relation to the radiation direction and the system's signal/noise ratio.

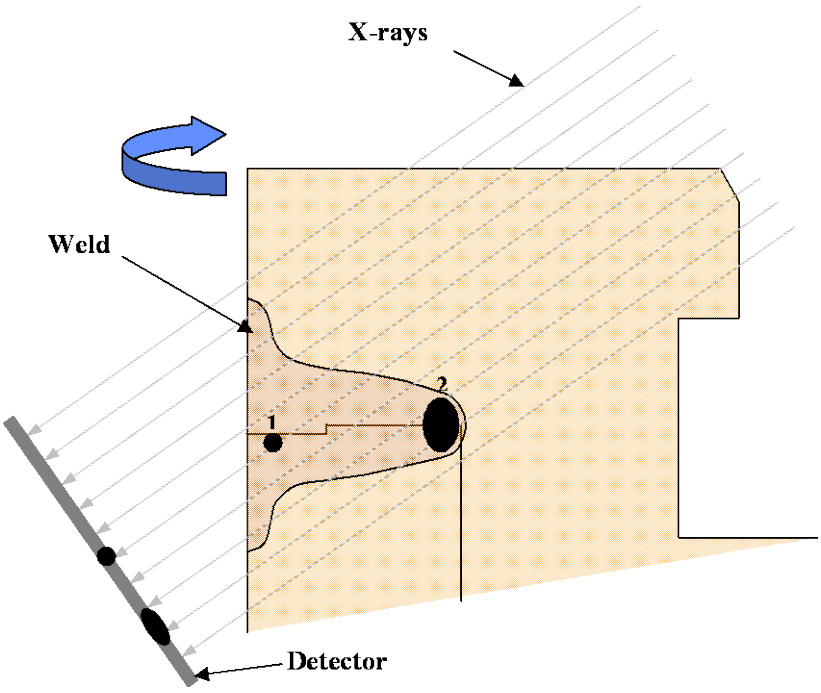

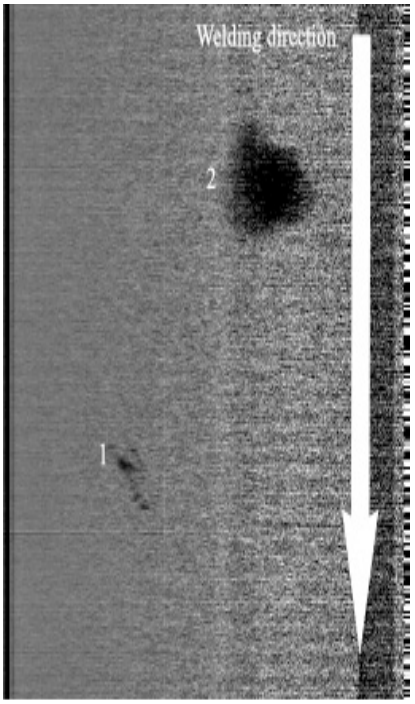

Figure 5-5. *Schematic illustration of radiographic testing of weld.* ***Figure 5-6.*** *Radiograph.*

The numbers in the figure above show where the indications in the radiograph at the right are located in the weld. The vertical axis represents the welding direction with the start point at the top. To compensate for the large variations in copper thickness in the beam path, a mean value calibration is performed.

6 Description of possible defects

This chapter describes the defects that have been shown possible to generate with FSW in 5 cm thick copper. A more detailed description of the possible defects in the weld is provided in the report /SKBdoc 1175162/.

The defects described below occur in many cases only under extreme conditions (outside process window), while others are more common. A number of approaches have been used to catalogue the possible defects:

- Indications from NDT of welds performed at the Canister Laboratory have been examined, as well as welds from the development work at TWI. The indications have been verified by metallographic examination.
- Examinations of areas where the welding process has been outside the process window. Pieces have been cut out in selected areas for further study by radiographic examination, and in certain cases also by metallography.
- Randomly selected samples have been examined by microfocus X-ray inspection, followed in some cases by metallographic examinations.
- Furthermore, a number of metallographic examinations by independent laboratories have provided information on above all tiny defects or other anomalies not detected by NDT.

Of the defects described, only some occur in connection with welding with variables and responses inside or close to the process window. They are also described in Chapter 8.

There is at present no specific classification system for defects for FSW. The possible defects have therefore been classified according to the system deemed to be the closest, which applies to geometric imperfections in metallic materials associated with pressure welding /SIS, 2002/.

Table 6-1. Classification of defects.

Reference SS-EN-ISO 6520 (ISO 6520-2:2001)	Designation and explanation	Illustration
P 403	**Insufficient fusion** Insufficient fusion in the joint.	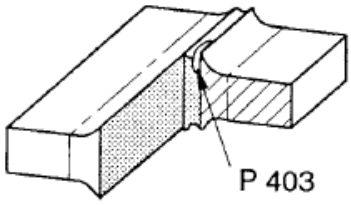
P 2013	**Localized porosity** Evenly distributed group of pores.	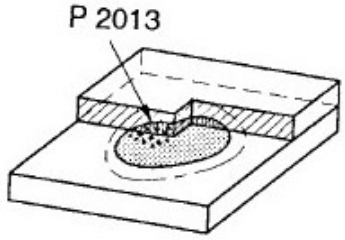

Reference SS-EN-ISO 6520 (ISO 6520-2:2001)	Designation and explanation	Illustration
P 2016	**Wormhole** A tubular cavity in the weld metal, generally grouped in clusters and distributed in a herringbone formation.	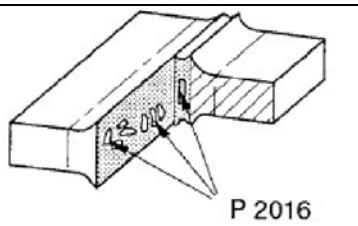
P 303	**Oxide inclusion** Thin metallic oxide inclusions in the weld (isolated or clustered).	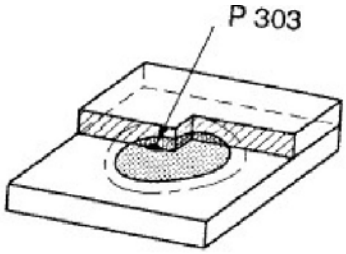
P 304	**Metallic inclusion** A particle of foreign metal trapped in the weld metal.	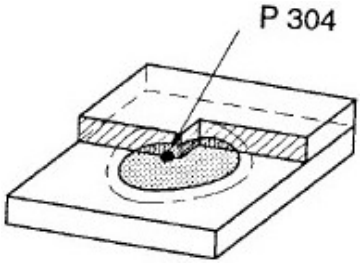

6.1 Defects detectable by NDT

In the trials with FSW at the Canister Laboratory, two types of defects in particular have been indicated: joint line hooking, JLH (P 4013) and wormholes (P 2016), see Figure 6-1.

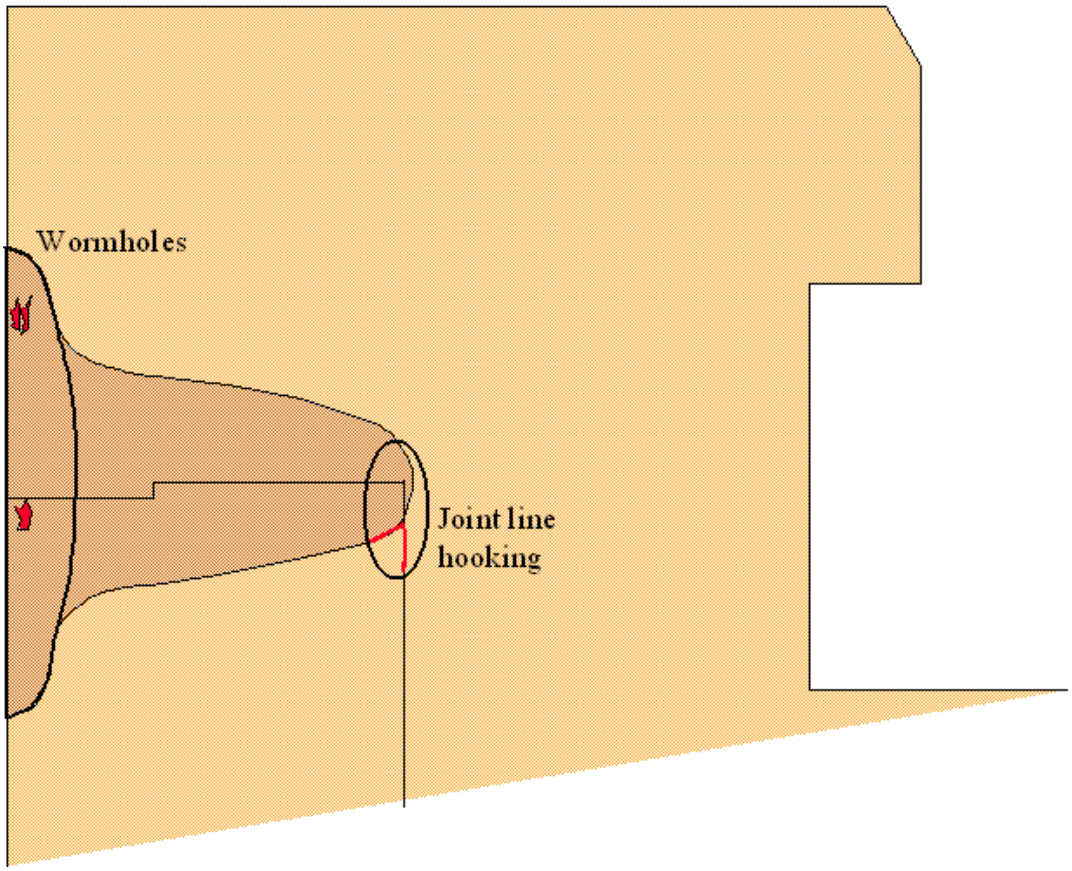

Figure 6-1. *Location of defects in welds.*

Joint line hooking (insufficient of fusion) ISO 6520-2:2001 P. 403

Joint line hooking, JLH, (see Figure 6-2) can occur in the internal part of the weld as a consequence of bending of the vertical joint between the tube and the lid during welding. The detectability of this type of defect is very good with ultrasound (see Figure 6-3), while it cannot be detected by radiography.

Description: The joint between the inside of the tube and the lid is bent towards the tool shoulder due to the flow of material around the tool probe.

Size: Up to 5.5 mm extent in radial direction has been noted. Normally, JLH has a tangential extent of one or two decimetres. However, in extreme cases these defects may extend along the entire weld revolution.

Location: In the weld root.

Characteristics: Dense crack-like defect with extent in radial direction with a gap of <10 µM, angle radial/axial <20º. Good surface finish.

Occurrence: At the overlap sequence (see Figure 3-3) in all lid welds.

Importance for properties in the weld metal: Reduces the corrosion barrier.

Cause: The flow of material causes the vertical joint line to be pulled out in the horizontal direction. The size of the JLH is linked to the penetration of the tool probe.

Prevention: JLH can be minimized (see also section 8.6) by reducing the flow of material in the area by reducing the depth of penetration of the tool probe or by changing the flow direction of the material by changing the welding or rotation direction.

Testing method: Ultrasonic testing from the top of the lid with the sound direction in the range ±20º.

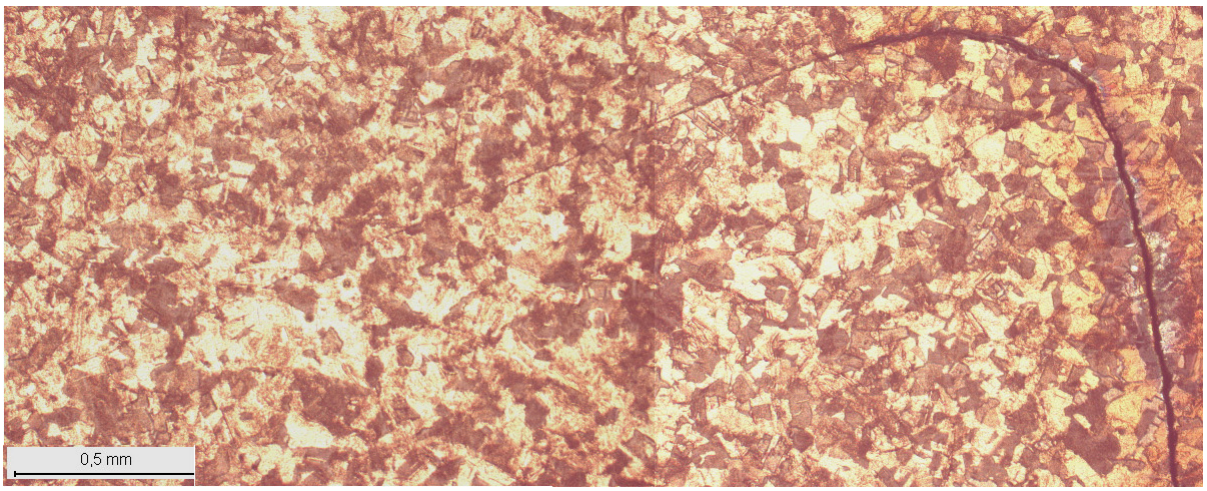

Figure 6-2. *Macrospecimen of JLH.*

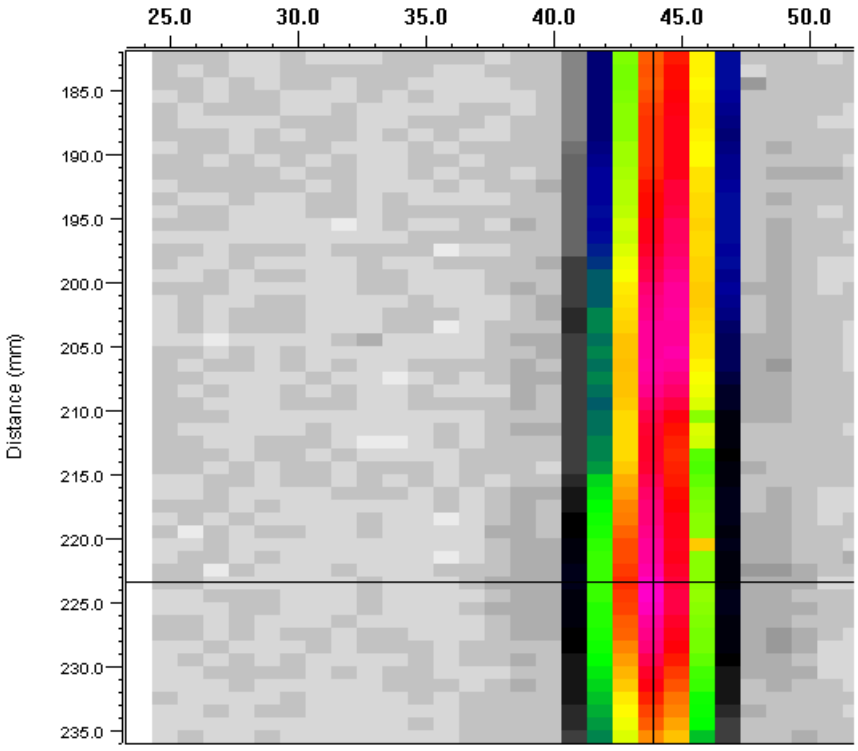

Figure 6-3. *Indications of JLH obtained in ultrasonic testing.*

Wormhole ISO 6520-2:2001 P. 2016

Wormholes (see Figure 6-4) can occur in the outer part of the weld as a consequence of welding variables outside the process window. The detectability of this type of defect is good with ultrasound (see Figures 6-5 and 6-6) but it can only be detected by radiography in the extreme case when it forms a volumetric defect.

Description: Near-surface defect that arises on the advancing side of the tool /Cederqvist, 2006/, which can also break the surface during the acceleration sequence.

Size: Up to 10 mm extent in radial direction has been noted when welding variables are outside the process window. The extent in the tangential direction is less than 10 mm, although clusters of defects can have a much greater tangential extent.

Location: Has been detected from the surface down to a depth of 10 mm.

Characteristics: Irregular shape with uneven surfaces. Usually consists of clusters with dense defects in the tangential direction with a primary extent in the radial/axial direction. In some cases when the welding variables are far from the process window, wormholes may merge into volumetric defects.

Occurrence: Large defects were found early in the development of the welding process, but only small defects (<3 mm) have been indicated in more recent welds.

Importance for properties in the weld metal: Reduces the corrosion barrier.

Cause: Welding variables, low shoulder depth and/or low tool temperature, outside the process window.

Prevention: Welding variables inside the process window.

Testing method: Visual in the case of surface-breaking defects, phased array ultrasound from the top of the lid with the sound field directed in the interval 0-30º and radiography of volumetric defects.

Figure 6-4. *Macrospecimen of volumetric wormhole.*

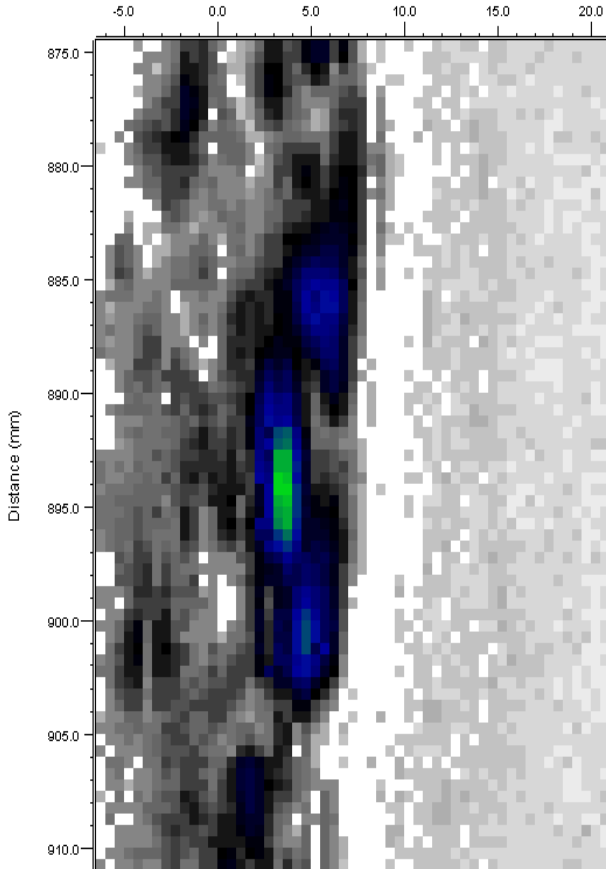

Figure 6-5. *Indications of wormhole obtained in ultrasonic testing.*

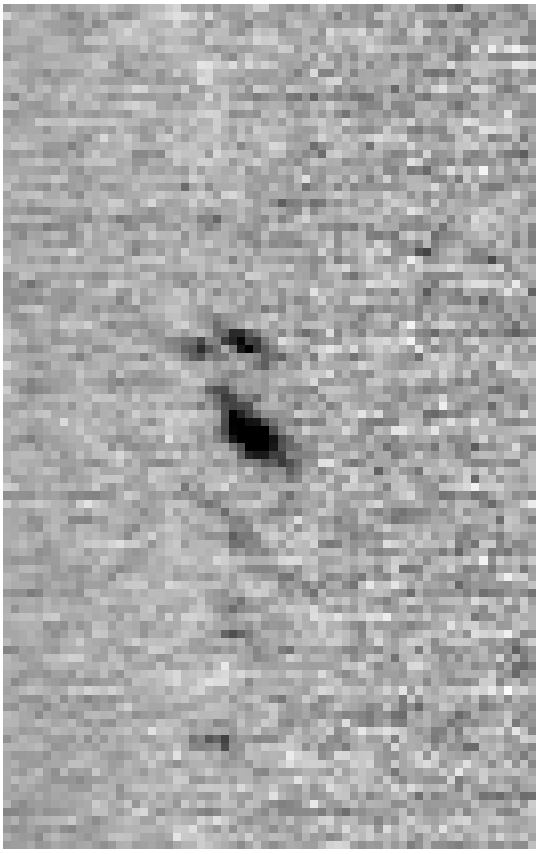

Figure 6-6. *Indications of wormhole obtained in radiographic testing.*

6.2 Defects not detectable by NDT

The probability of detection (POD) in all NDT decreases as the size of the defects decreases. Certain defects may have unfavourable characteristics for certain testing methods, making them difficult to detect. In order to get an idea of the occurrence and frequency of defects not detected by NDT, supplementary examinations were made.

6.2.1 Supplementary examinations

In the supplementary examinations, microfocus X-ray and metallographic examinations were performed on samples taken at random.

Microfocus X-ray

Microfocus X-ray was performed for the purpose of examining the possible occurrence of defects larger than 0.1 mm. The examinations /SKBdoc 1175235/ were performed at BAM with a 320 kV Seifert X-ray tube. The examinations were performed by X-raying the specimens in two directions, see Figure 6-7.

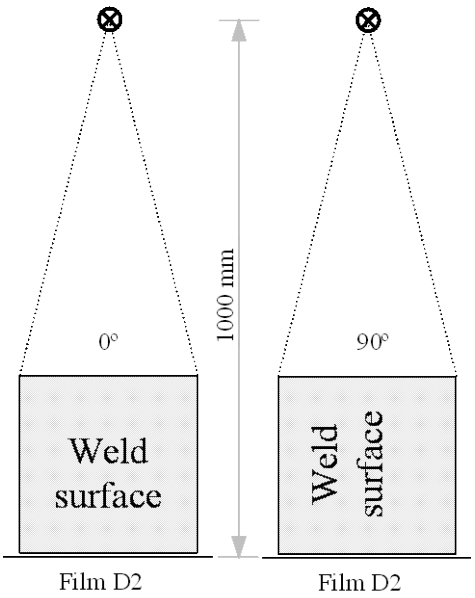

Figure 6-7. *Setup for microfocus X-ray.*

In the examinations, specimens were randomly cut out from all welds in the demonstration series. These specimens were then machined to bars (20x20x80) mm) suitable for examination in the radiography system.

The results of these examinations are presented in Chapter 8.

Metallographic examinations

As a complement to the microfocus X-ray examinations, various metallographic examinations were also performed. One round of examinations included thorough inspection of eight drill cores taken randomly from welds. The drill cores had a diameter of 40 mm and the examination was conducted by slicing up the material in 0.5 mm increments and examining the section surfaces visually. A total of 800 sections were studied. Furthermore, some 20-odd macrospecimens were taken out for more careful examination under a microscope. These examinations were supplemented by SEM examinations with EDS and refined microscopy.

The results of these examinations are presented in Chapter 8.

6.2.2 Description of defects

Three types of small defects were found in FSW welds.

- Pores and clustered porosities.
- Oxide inclusions.
- Metallic inclusions.

Clustered porosity ISO 6520-2:2001 P. 2013

Description: Single pores or pore strings.

Size: Strings up to 9 mm long were observed. The pores are around 0.1-0.5 mm in size.

Location: Found in all parts of the weld.

Characteristics: See Figure 6-8.

Occurrence: When welding was done inside the process window only single small pores were observed in certain welds.

Importance for properties in the weld metal: When welding is done inside the process window they have little effect on the effective corrosion barrier.

Cause: Clustered porosities arise when one or more welding variables are outside the process window. Single pores can arise at random.

Prevention: Make sure that welding is done inside the process window. Near-surface clustered porosities are often machined off when the lid is machined to its final dimensions.

Examination method: Can only be detected by metallographic examinations.

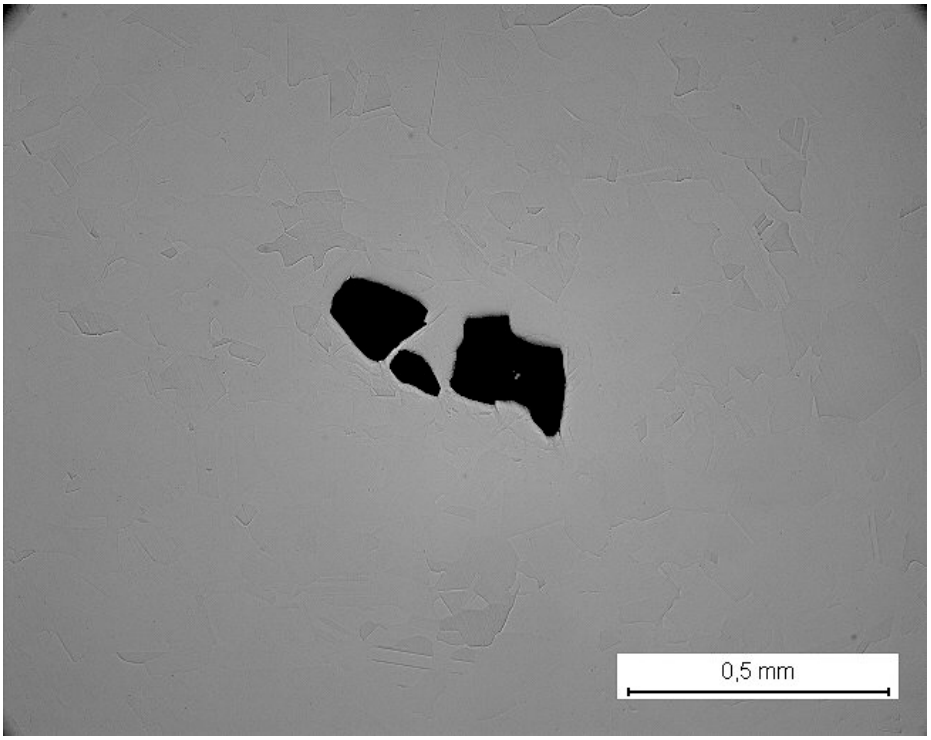

Figure 6-8. *Clustered porosity in overlap zone on lid weld 35.*

Oxide inclusions

Description: Copper oxide, see Figure 6-9.

Size: Oxides of length < 300 µm were detected.

Location: Normally occur near the surface in an area that is machined off.

Occurrence: Found in all examined lid welds, usually in the overlap sequence.

Importance for properties in the weld metal: Very little effect on the effective corrosion barrier.

Cause: If welding is done in an atmosphere with oxygen, copper oxidizes rapidly and the oxide is stirred into the weld metal.

Prevention: One lid weld produced in argon gas showed that oxide-free weld zones can be produced.

Examination method: Can only be detected by metallographic examinations.

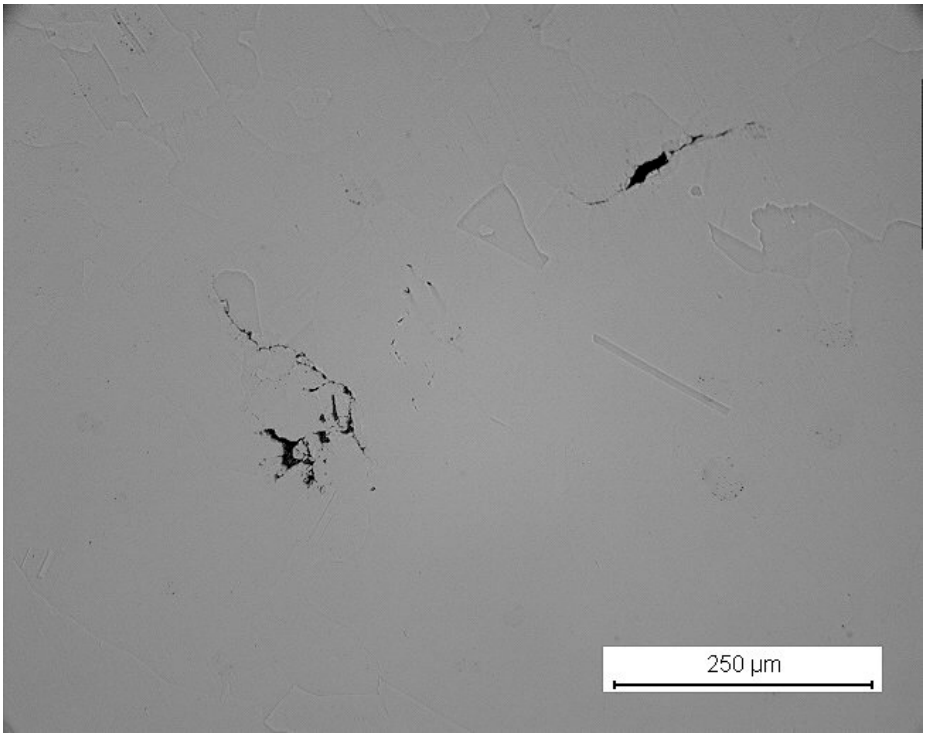

Figure 6-9. *Cluster of oxidized particles in the overlap zone on lid weld 36.*

Metallic inclusions

Description: Traces of tool material in the weld metal, se figure 6-10.

Size: Particles of length < 300 μm were detected.

Location: Usually near the surface but distributed throughout weld zone.

Occurrence: In all lid welds.

Importance for properties in the weld metal: Due to the small size of the particles, they are not expected to affect the corrosion barrier.

Cause: Tool wear.

Prevention: Surface treatment of tools has reduced trace levels. Corrosion tests show that metallic traces does not reduce the corrosion resistance /Gubner and Andersson, 2007/.

Examination method: Can be detected by high-sensitive radiography on cut-out specimens or by chemical analysis of the weld metal as elevated concentration of foreign metals.

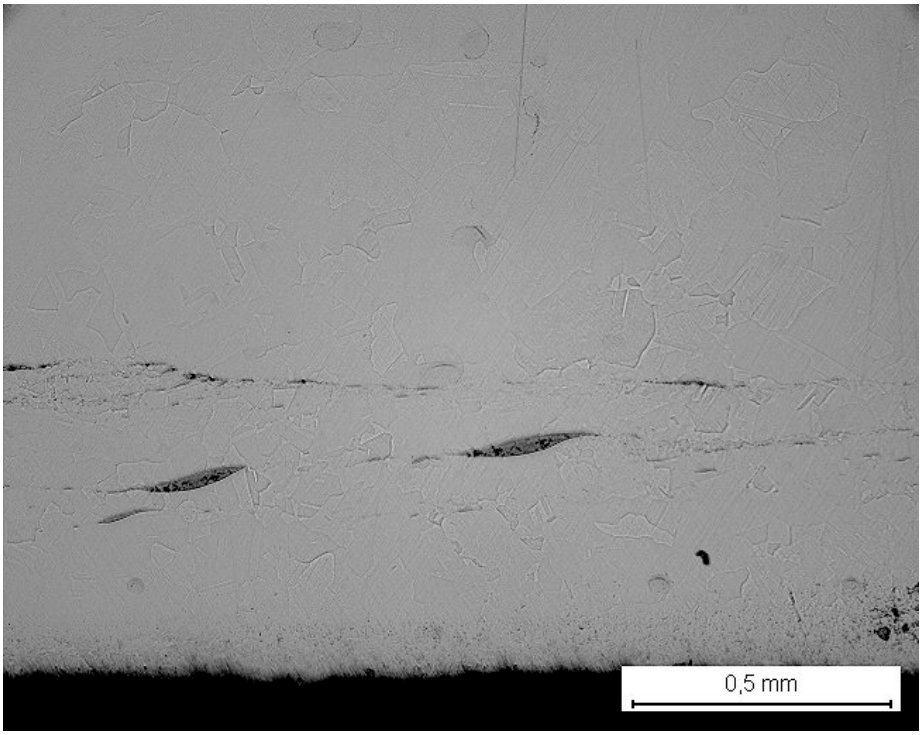

Figure 6-10. *Traces of foreign material (W) near-surface in unmachined lid weld 20.*

7 NDT reliability

A project was started in 2003 at BAM (Bundesanstalt für Materialforschung- und Prüfung) entitled "NDT Reliability" in order to determine the reliability of the NDT processes. The results of the project are outlined in this chapter. A more detailed description is provided in the data report /SKBdoc 1175235/ and in the project's final report /Müller C, et al, 2006/.

7.1 Background

An initial study to determine the ability of the NDT processes to detect and determine the size of defects was conducted in 2001 /Ronneteg and Moberg, 2003/. The study included 43 defects that had been indicated in electron beam welds where size estimated by ultrasound and radiography was compared with size estimated by metallographic examinations. The study showed good correlation between size estimated by NDT and measured size.

The "NDT Reliability" project at BAM included evaluation of NDT of welds made by both FSW and EBW for the purpose of determining POD (Probability of Detection), and precision in estimation of the size of defects.

7.2 Strategy

By "NDT reliability" is meant the ability to detect and determine the size of defects and to estimate the risk of false calls.

In order to determine the reliability of NDT processes, they can be divided into three parts (see Figure 7-1), where each part influences the reliability of the process:

- The intrinsic physical capability of the method to detect relevant defects for the process (IC).
- Technical application factors that influence the testing (AP).
- Effects of human factors (HF).

The goal in this project has been to determine the capability of the NDT process to detect and determine the size of defects, with a focus on the physical variables. Other application factors and human factors will be studied at a later stage when the technical solutions have been finalized. The goal is that these factors will be minimized in the design of processes and systems.

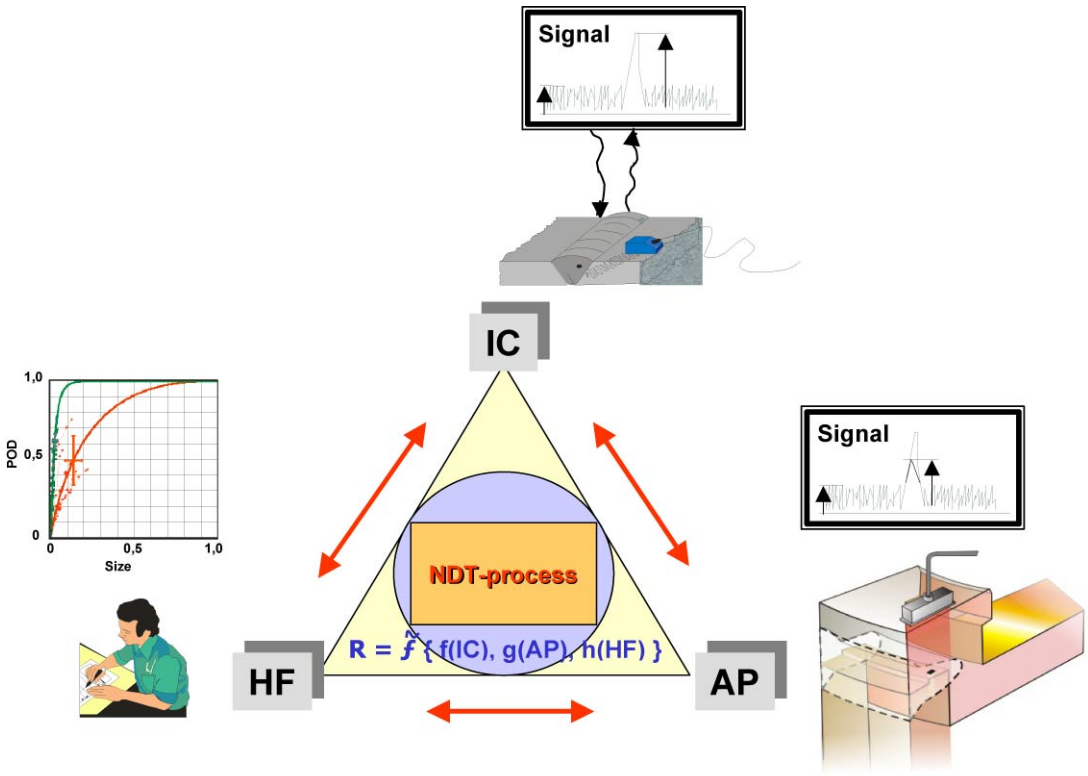

Figure 7-1. *NDT reliability, IC (intrinsic physical capability), AP (technical application factors), HF (human factors).*

The method that BAM used to determine the Probability of Detection (POD) of the NDT processes uses the ratio between signal strength $\hat{a}$ from the detection system and the size of the defect a, see Figure 7-2. The method is described in MIL-HDBK 1823 /US Department of defense, 1999/ and was developed for the USA's military space industry.

Figure 7-3 shows a POD curve where POD is plotted against the size of the defect. The value $a_{90/95}$ is used as a measure of POD though it can be stated as a reasonable high level. The indexation (90/95) indicates that 90% of the defects with size a will be detected within a confidence interval of 95%, i.e. the uncertainty in determination of the POD curve.

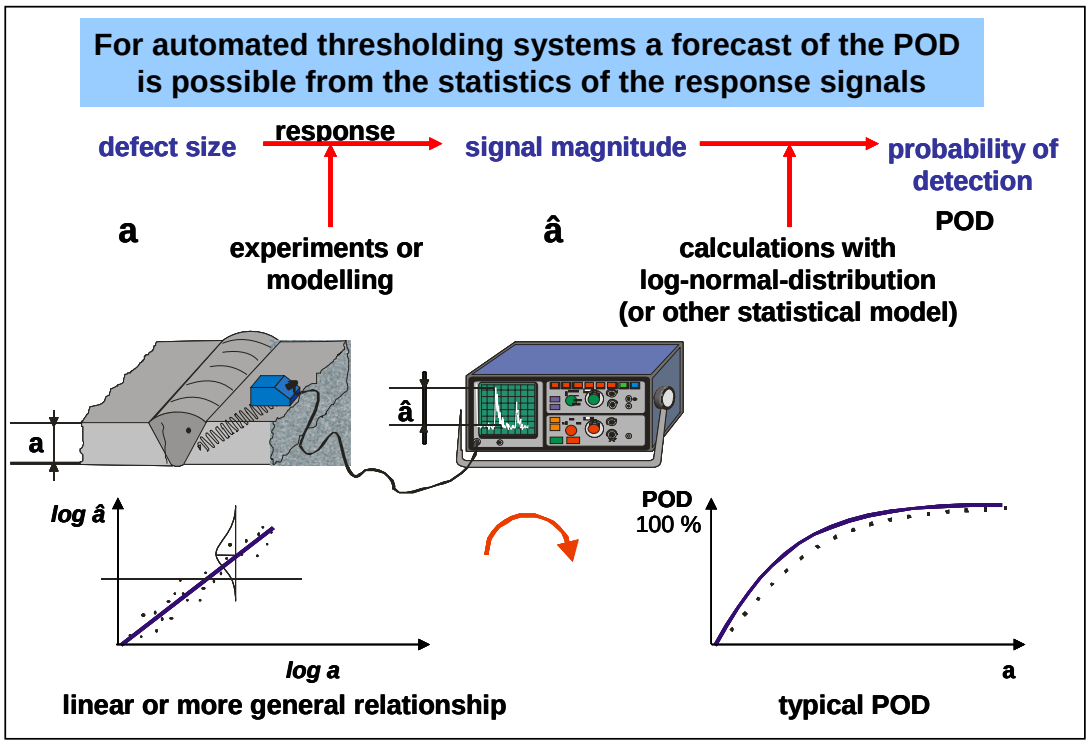

Figure 7-2. *General description of methodology for determination of POD.*

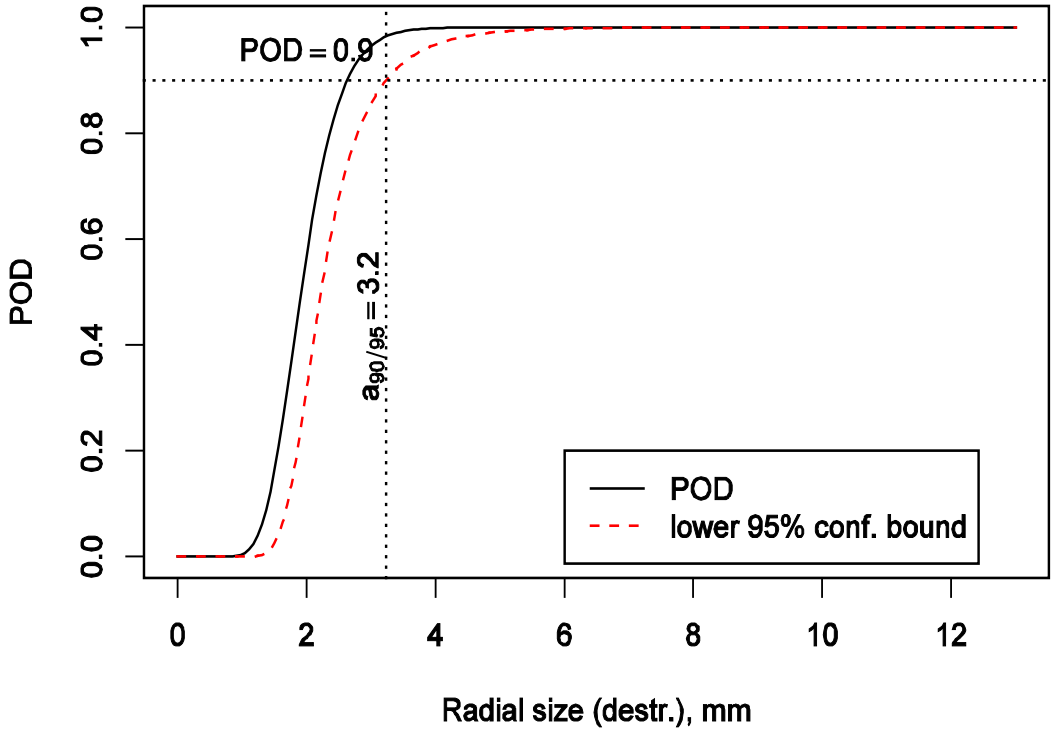

Figure 7-3. *Example of POD curve where 95% lower confidence bound crosses 90% POD.*

7.3 Practical procedure

In order to obtain suitable specimens, welds were performed where as the processes were intentionally disturbed. Examples of disturbances in the welds are contamination and damage to joint surfaces and deviation from normal process variables. The purpose was to generate a large number of different defects that could arise in the processes. Furthermore, supplementary material from other welds was used to provide a large enough body of statistics for the analysis.

The welds were examined by NDT according to the Canister Laboratory's procedures for radiographic and ultrasonic testing. Specimens and examination results from NDT were delivered to BAM, where the specimens were examined by different reference methods: HECT (High Energy Computed Tomography) and μ-CT (Microfocus Computed Tomography). Supplementary evaluation was also done at the Canister Laboratory. Finally, metallographic examinations were also carried out to verify the occurrence, shape and extent of the defects.

7.4 Results

The results of the reliability study include the capability of the NDT process to detect (POD) and determine the size of different types of defects.

7.4.1 Probability of Detection, POD

In the case of wormhole-type defects, it has not been possible to obtain a direct relationship between signal size and radial size of the defects. In the case of radiography, first a value of $a_{90/95}$ for penetrated thickness was determined with HECT (Figure 7-4). Then this value was correlated to the actual size of the defects (Figure 7-5), giving a value of 4 mm for a_r. Further studies /Müller C, et al, 2006/ show however that optimized threshold levels from radiographic evaluation can improve these values. It should also be noted that the defects used in this study were generated in welds with weld variables outside the process window and that they are thereby volumetric. In the case of ultrasound, first a value of $a_{90/95}$ was determined for the reflected area of the defects in immersion testing (Figure 7-6). Then this value was correlated to the actual size of the defects (Figure 7-7), giving a value of 6.3 mm for a_r.

In the case of defects of the JLH type, a direct relationship between signal strength and the radial size of the defects was used as a consequence of the fact that the tangential extent is much greater than the sound field in this direction. These specimens exhibit a POD $a_{90/95}$ of 4.0 mm, see Figure 7-8.

The results are compiled in Table 7-1, while a more detailed discussion is presented in the report where all data are presented /SKBdoc 1175235/.

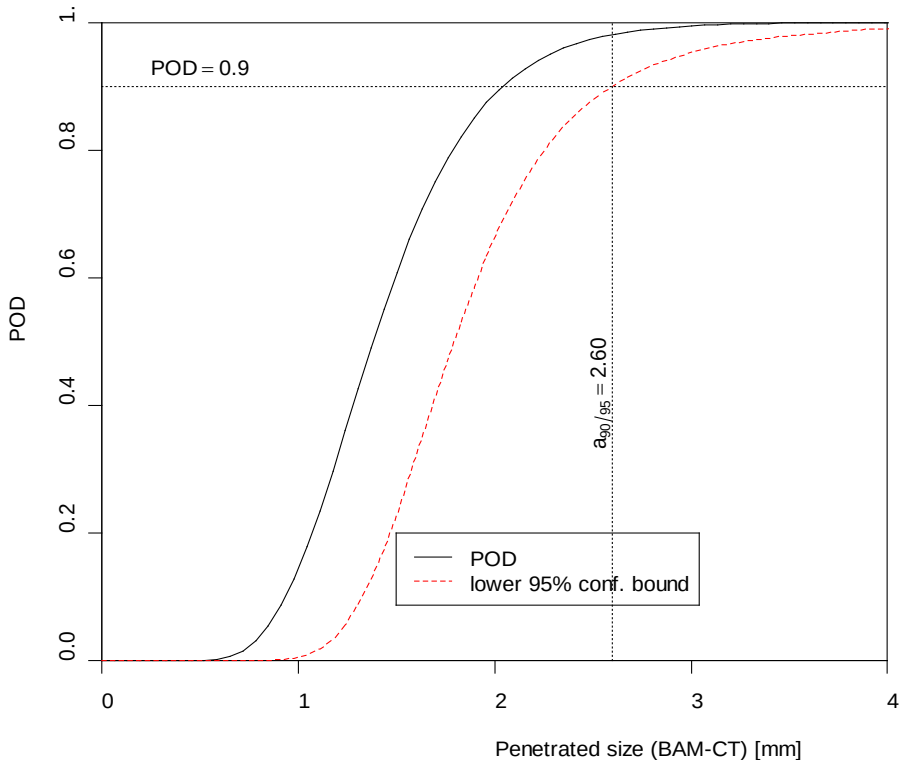

Figure 7-4. *POD for radiographic testing of wormhole.*

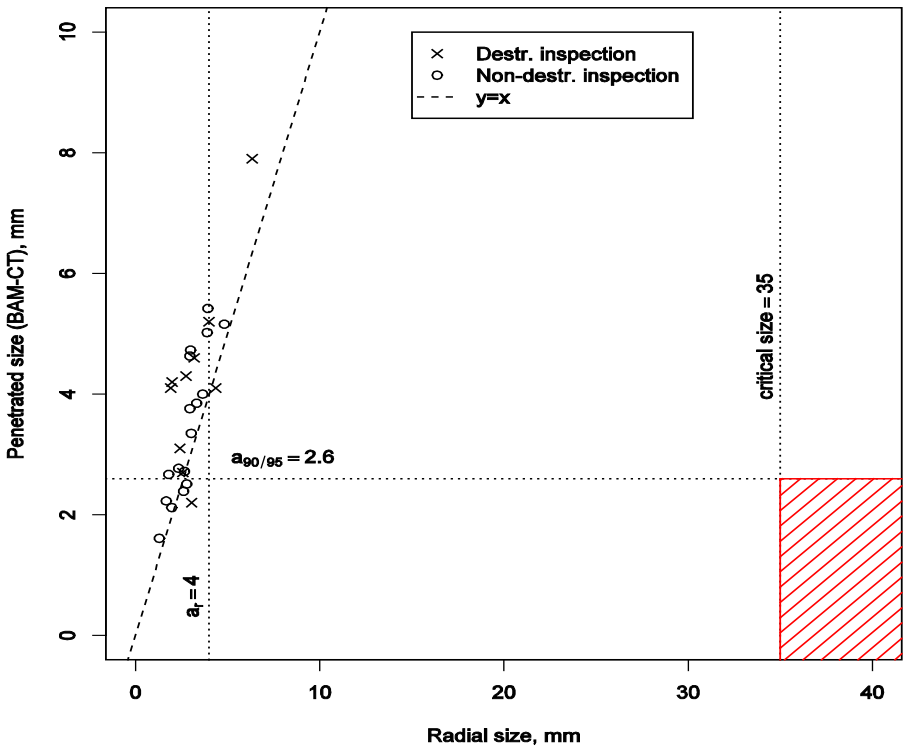

Figure 7-5. *Scatter plot for radiographic testing of wormhole.*

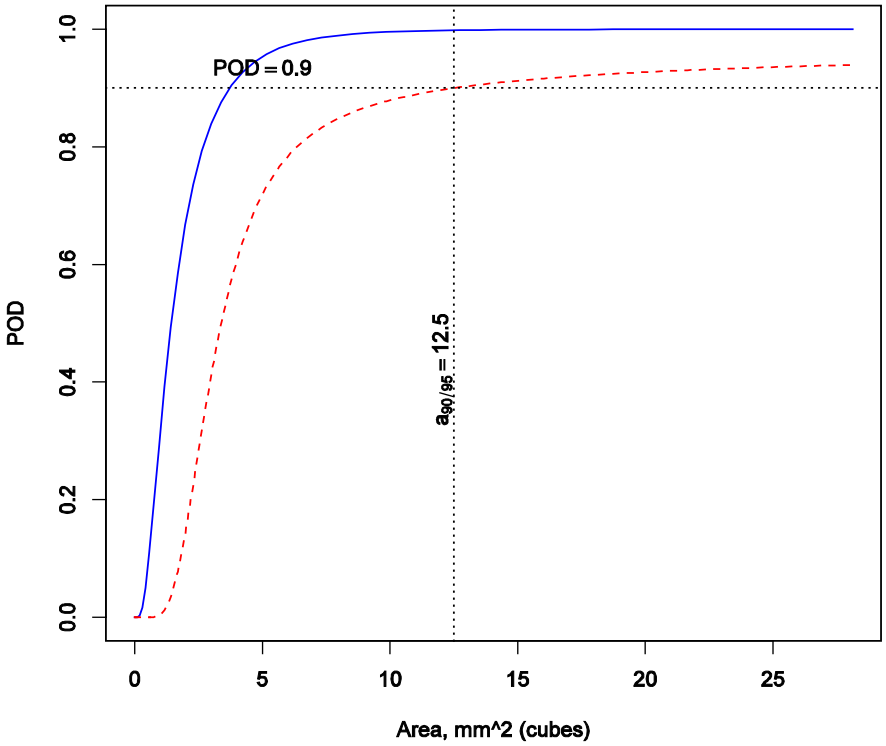

Figure 7-6. *POD for ultrasonic testing of wormhole.*

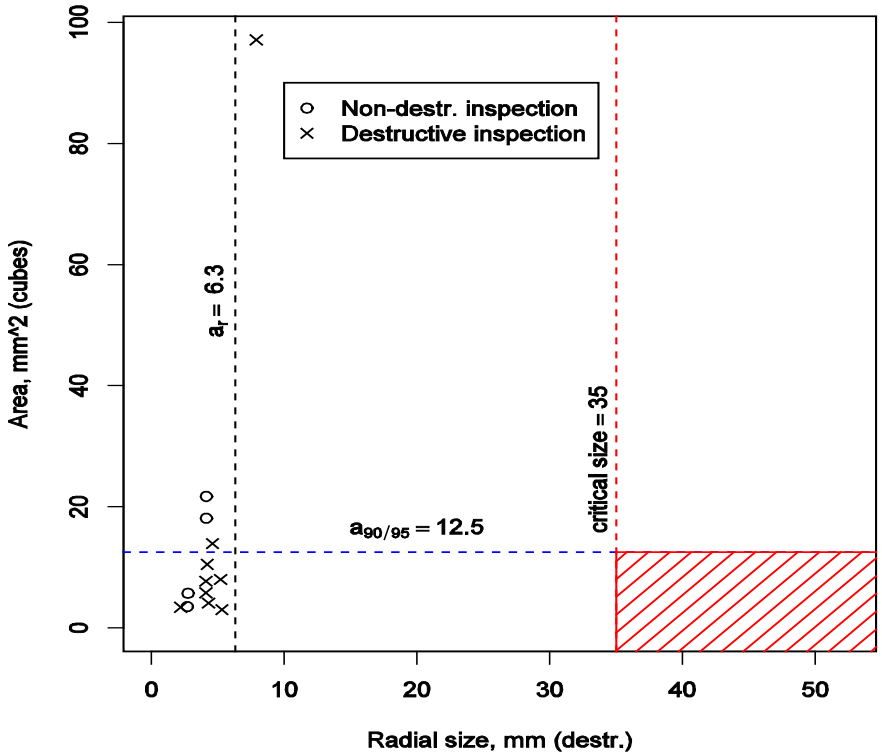

Figure 7-7. *Scatter plot for ultrasonic testing of wormhole.*

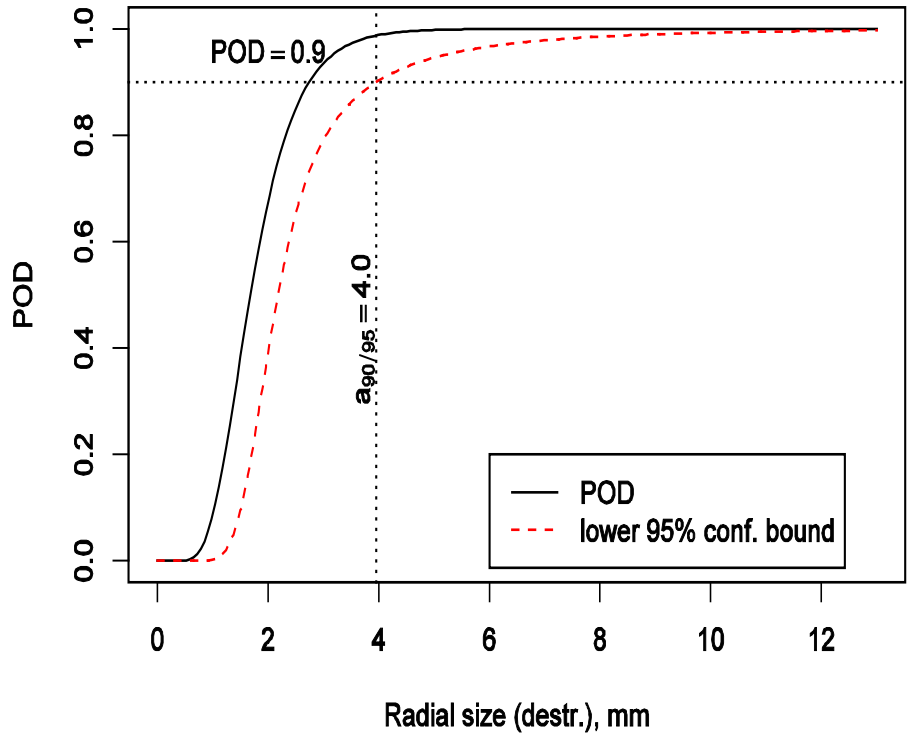

Figure 7-8. *POD for ultrasonic testing of joint line hooking.*

Table 7-1. POD results for FSW

	$a_{90/95}$ UT (mm)	$a_{90/95}$ RT (mm)
Wormhole	6.3 mm	4.0 mm
JLH	4.0 mm	

7.5 Accuracy in size estimation

The measurement error in non-destructive testing can be estimated with a reference method (destructive test). Input data, size estimated by NDT and size estimated by destructive testing, as well as measurement error (the difference), are presented in Tables 7-2, 7-3 and 7-4. The distribution of the measurement errors is shown by frequency histograms in Figures 7-9, 7-10 and 7-11.

Table 7-2. Measurement error with ultrasonic testing, a comparison with destructive testing with regard to indications of JLH.

Test	Size, UT (mm)	Size, reference (mm)	Measurement error (mm)
1	4.0	3.3	0.7
2	4.0	5.4	-1.4
3	4.0	3.3	0.7
4	4.5	4.5	-0.0
5	4.0	4.8	-0.8
6	3.0	2.6	0.4
7	4.0	3.3	0.7
8	3.5	4.2	-0.7
9	4.0	4.1	-0.1
10	4.5	4.2	0.3
11	4.0	3.5	0.5
12	3.5	3.0	0.5
13	3.5	2.4	1.1
14	3.0	1.8	1.2
15	3.0	1.7	1.3
16	2.5	2.0	0.5
17	4.0	4.7	-0.7
18	3.0	3.9	-0.9
19	4.0	1.5	2.5
20	3.0	1.4	1.6
21	4.0	2.8	1.2
22	4.0	4.1	-0.1
23	4.0	2.7	1.3

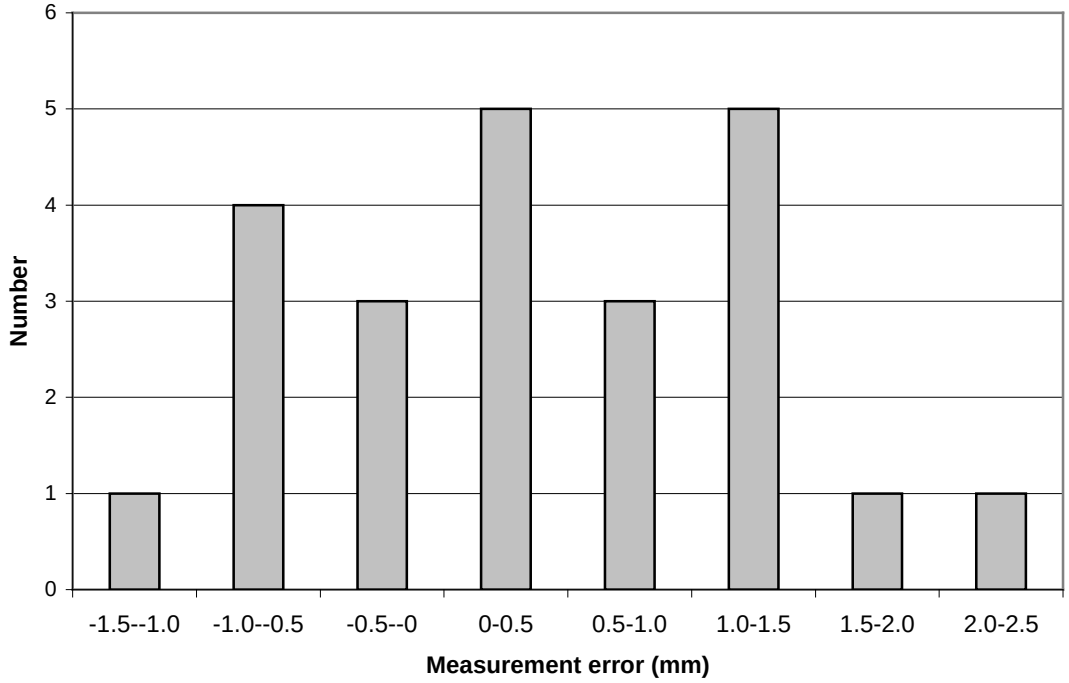

Figure 7-9. *Histogram of measurement error for UT of JLH.*

Table 7-3. Measurement error with ultrasonic testing, a comparison with destructive testing with regard to indications of wormholes.

Test	Size, UT (mm)	Size, reference (mm)	Measurement error (mm)
1	5.0	5.3	-0.3
2	6.5	7.9	-1.4
3	2.5	2.7	-0.2
4	2.0	4.1	-2.1
5	4.0	2.8	1.2
6	2.0	4.1	-2.1
7	3.0	4.3	-1.3
8	2.5	4.2	-1.7
9	2.5	3.1	-0.6
10	2.0	2.2	-0.2
11	4.5	5.2	-0.7
12	5.0	4.6	0.4

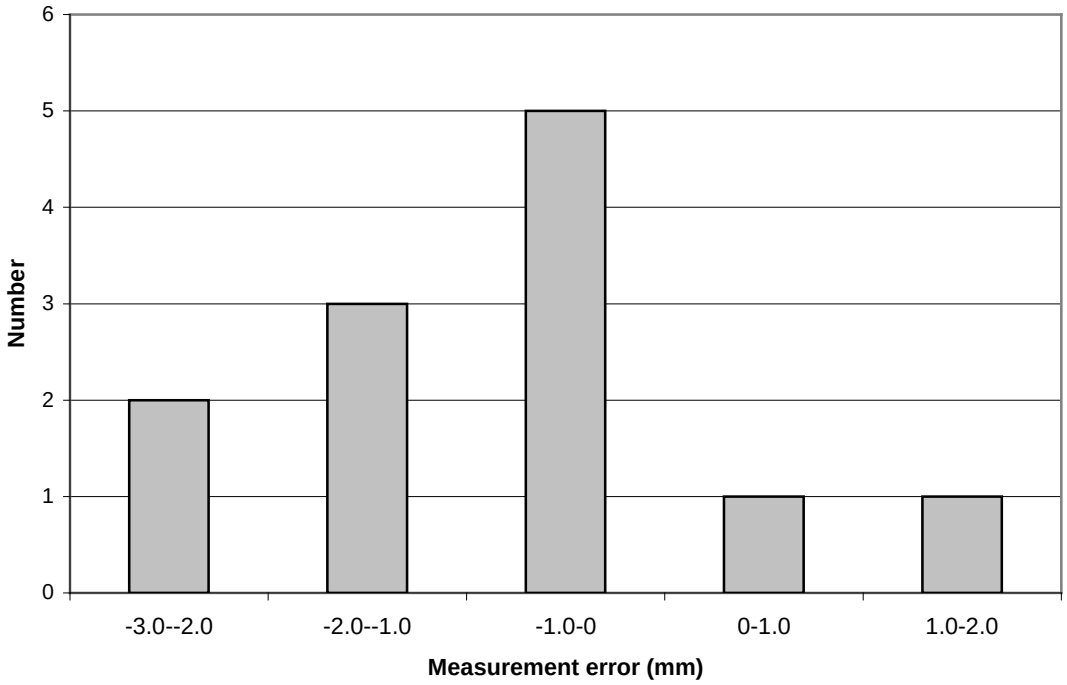

Figure 7-10. *Histogram of measurement error for UT of wormholes.*

Table 7-4 Measurement error with radiographic testing, a comparison with destructive testing with regard to indications of wormholes.

Test	Size, UT (mm)	Size, reference (mm)	Measurement error (mm)
1	5.5	5.3	0.2
2	13.8	7.9	5.9
3	1.8	2.7	-0.9
4	5.0	4.1	0.9
5	1.7	4.1	-2.4
6	2.4	4.3	-1.9
7	3.0	4.2	-1.2
8	3.0	3.1	-0.1
9	5.3	5.2	0.1
10	4.4	4.6	-0.2

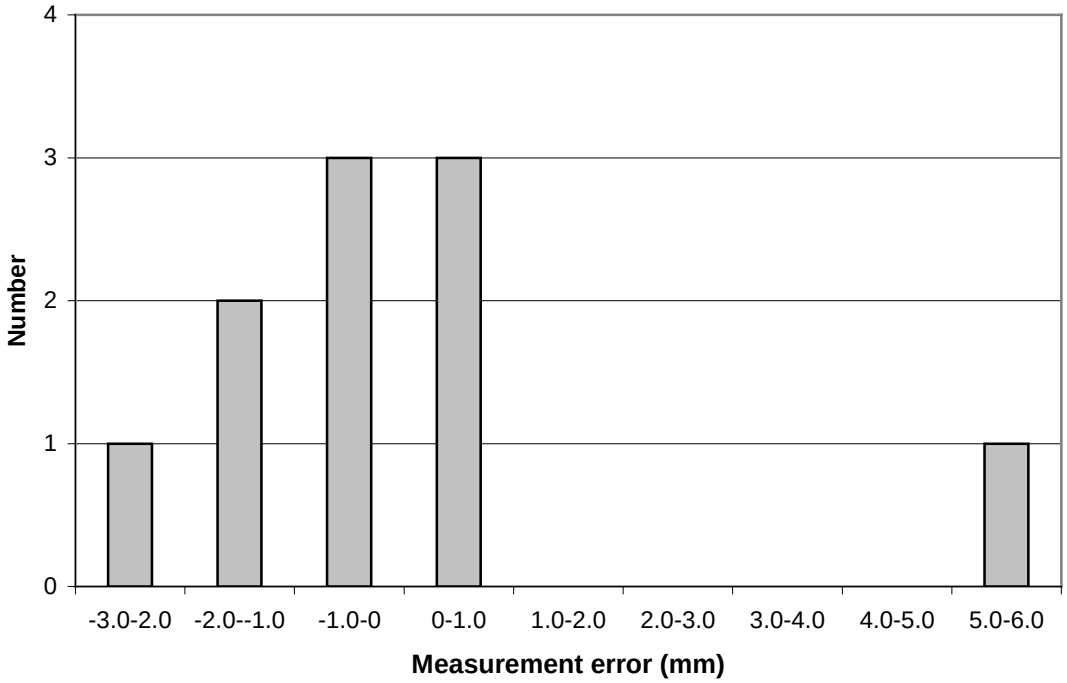

Figure 7-11. *Histogram of measurement errors for RT of wormholes.*

Estimated uncertainty interval

As regards JLH-type defects, the results show that the mean value for the measurement errors is 0.426 with a standard deviation of 0.929. A two-sided 95% confidence interval for the mean value calculated with re-sampling (Efron's percentile method) varies from 0.056 to 0.796 mm /Efron and Tibshirani, 1993/. The maximum measurement error is an overestimation of the defect size by 2.5 mm (test 19 in Table 7-2 above).

The measurement error for JLH-type defects is size-dependent and exhibits a clear relationship with the defect size indicated from the reference method, Figure 7-12. The size of small defects (<3 mm) is overestimated by NDT and larger defects (>4 mm) are underestimated. A similar relationship does not exist with the measured defect size, which means the NDT results cannot be simply corrected to eliminate the systematic error.

As regards wormhole-type defects measured by ultrasound, the results show that the mean value for the measurement errors is -0.750 with a standard deviation of 1.010. A two-sided 95% confidence interval

for the mean value calculated with resampling varies from -1.128 to -0.192 mm. The maximum measured measurement error is an underestimation of the size by 2.1 mm (tests 4 and 6 in Table 7-3 above).

As regards wormhole-type defects measured with radiography, the results show that the mean value for the measurement errors is 0.040 with a standard deviation of 2.293. A two-sided 95% confidence interval for the mean value calculated with resampling varies from -1.090 to 1.550 mm. The maximum measured measurement error is an overestimation of the size by 5.9 mm (test 2 in Table 7-4 above).

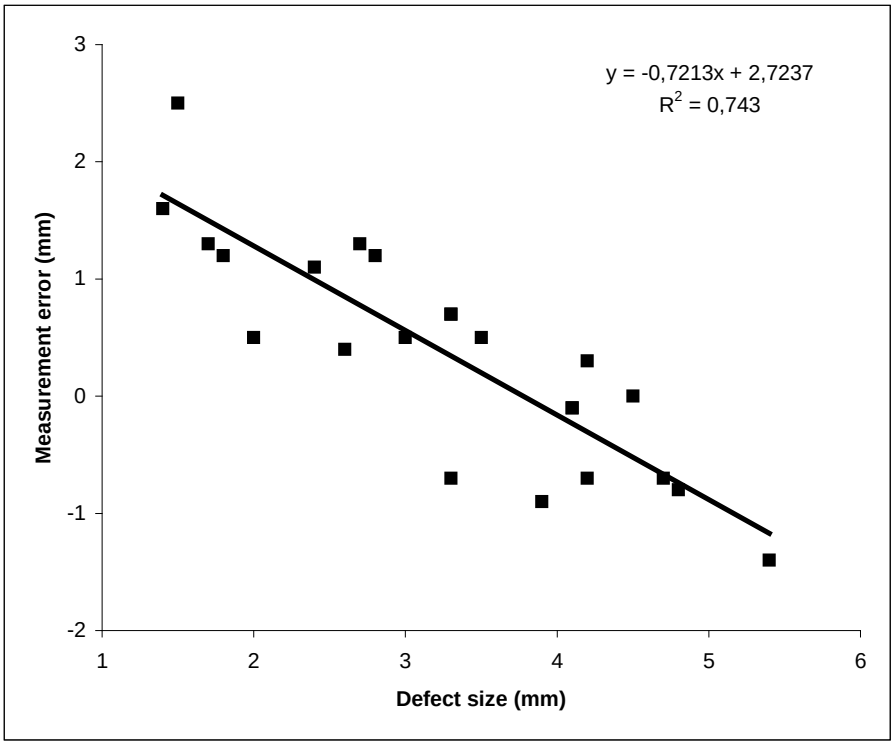

Figure 7-12. *Measurement error with ultrasound as a function of defect size determined by destructive testing (mm).*

8 Demonstration and post-demonstration series

As mentioned in chapter 1, the purpose of the demonstration series was to show the weld quality that can be achieved under production-like forms and to show that the welding process and the welding system can be operated in serial production. The demonstration programme was carried out in late 2004 and early 2005 and consisted of 20 lid welds.

In the fall of 2006 a so-called post-demonstration series was produced to display the status of the improved welding procedure with respect to the size of the JLH. In this experiment, a probe of shorter (optimized) length was used and the occurrence of JLH defects was evaluated with NDT and destructive testing. The post-demonstration series contained 20 shorter weld segments produced on 2 lids. The shorter weld segments were used with a start above the joint line, down-travel, approximately 30˚ of joint line welding, and an overlap of the previous segment and park.

8.1 Evaluation of process and system

All 20 welds in the demonstration series were carried out under production-like forms. No tests of the system or the process needed to be carried out in addition to the lid welds. In other words, the demonstration series could be carried out without interruption, which shows that process and system have high reliability and availability.

Table 8-1 shows mean, minimum and maximum values as well as standard deviations for the welding factors during a complete revolution (360 degrees in the X direction) of joint line welding for all lid welds in the demonstration series. Equivalent results for the welding responses, tool temperature and shoulder depth, are presented in Table 8-2. However, shoulder depth was only checked at the start of the downward sequence. The parking sequence (Figure 3-3) is begun by a manual command, which leads to just over 360 degrees of joint line welding. The part of the weld that is overlapped is thus not included in the analysis of the process window. Figure 8-1 shows the tool temperature over these 360 degrees of joint line welding for all 20 welds.

Table 8-1. Welding factors in demonstration series.

	Spindle speed (SS)				Welding force (FZ)			
Weld ID	**Mean**	**Min.**	**Max.**	**St. dev.**	**Mean**	**Min.**	**Max.**	**St. dev.**
22	405	370	436	12.9	84.9	80.0	91.3	2.3
23	403	370	437	15.2	84.7	80.6	92.6	2.2
24	393	360	442	17.0	84.1	79.5	90.8	2.2
25	409	385	442	14.4	84.9	80.5	94.3	2.4
26	410	390	436	10.6	85.0	81.0	91.3	2.2
27	397	375	432	11.4	84.7	80.7	93.7	2.3
28	384	355	442	14.0	84.0	79.7	91.2	2.3
29	405	377	419	9.0	84.5	79.8	94.5	2.4
30	395	357	434	15.0	84.7	80.8	91.5	2.2
31	396	357	424	14.3	85.5	80.9	93.3	2.4
32	398	377	429	11.6	86.2	80.3	94.5	2.6
33	399	367	429	13.0	85.8	81.0	93.1	2.4
34	392	372	444	15.9	86.9	81.6	94.8	2.5
35	398	367	443	11.4	86.8	81.2	93.6	2.5
36	407	387	434	8.9	86.3	81.0	93.2	2.5
37	385	362	429	10.5	88.3	82.6	93.7	2.5
38	400	377	428	11.0	88.0	82.4	95.5	2.5
39	379	357	398	7.4	84.4	79.4	90.0	2.2
40	379	352	414	15.3	87.3	82.3	93.0	2.4
41	388	357	444	15.6	87.8	83.0	94.3	2.4
Mean	396	369	432	12.7	85.7	80.9	93.0	2.4

Table 8-2. Welding responses in demonstration series.

	Tool temperature (TT)				Shoulder depth (PZ)
Weld ID	**Mean**	**Min.**	**Max.**	**St. dev.**	
22	861	836	879	7.0	0.8
23	859	825	881	11.8	1.3
24	859	828	874	5.3	1.1
25	856	831	868	5.9	1.1
26	856	844	873	4.9	0.8
27	857	831	876	6.0	1.1
28	854	826	899	7.0	1.2
29	854	835	878	5.8	1.2
30	855	829	874	6.3	0.8
31	855	839	871	4.9	1.0
32	854	829	867	5.7	1.1
33	854	839	866	4.9	1.0
34	853	817	864	7.1	1.2
35	854	828	869	5.2	1.3
36	851	821	865	7.6	1.0
37	853	838	873	5.1	0.7
38	851	824	867	6.3	1.0
39	853	835	885	5.8	1.1
40	854	836	872	4.7	1.0
41	850	798	877	10.6	1.6
Mean	854	829	874	6.4	1.1

Figure 8-2 shows how the position of the different lid welds compared with the process window at the start of the downward sequence (Figure 3-3).

The demonstration series has shown that the process that has been developed and optimized is robust and repeatable. The process could be run within the tested process window (see Table 4-8 in Chapter 4.3) with good margin. It was, however, noted that one weld (ID 41) had a shoulder depth of 1.6 mm (process window 0.4-1.5 mm) when the downward sequence started. The process was adjusted to correct this, which caused the tool temperature to fall to 778°C (process window 790-910°C) for a brief period. The area where this happened was, however, within the overlap zone and was thereby automatically rewelded, this time with variables inside the process window (Table 8-2 and Figure 8-1).

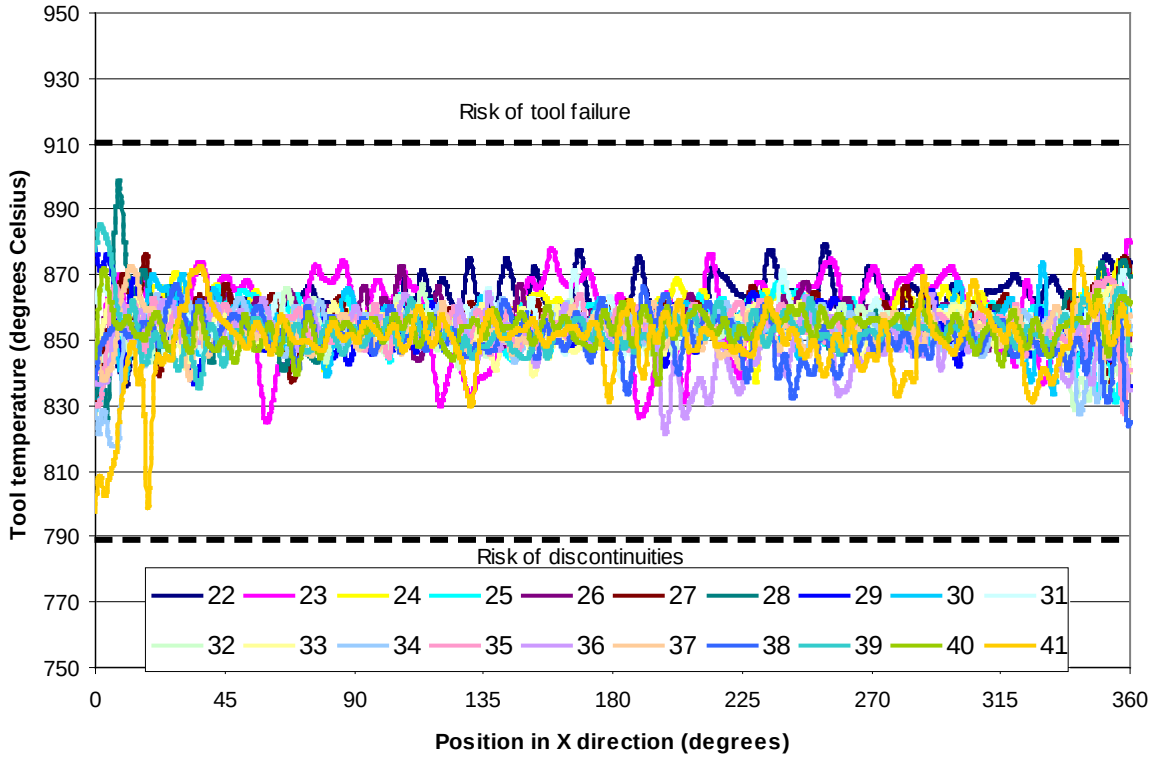

Figure 8-1. *Tool temperature during 360 degrees of joint line welding with weld ID.*

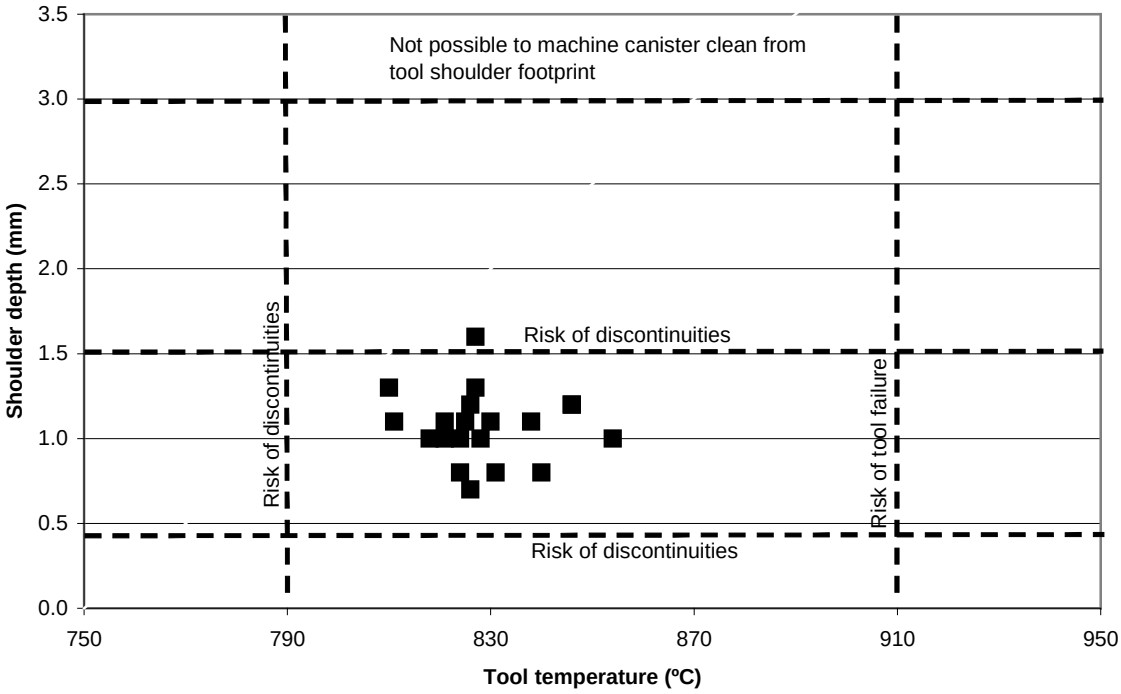

Figure 8-2. *Process window for the weld responses with data from the demonstration series.*

8.2 Evaluation of demonstration series with NDT

All 20 welds in the demonstration series were examined by non-destructive testing both before and after machining. The testing before machining was used to verify that correct settings had been used in the welding process. After machining, all welds were examined by both phased array ultrasonic testing and digital radiography according to the Canister Laboratory's procedures.

No volumetric defects were detected by digital radiography. A total of 54 defects were indicated by ultrasonic testing. Joint line hooking was indicated in all welds with a radial extent in the range 2-5 mm, see distribution in Figure 8-3. Verifying destructive testing was performed in order to determine the true radial size of the defects /SKBdoc 1046524/.

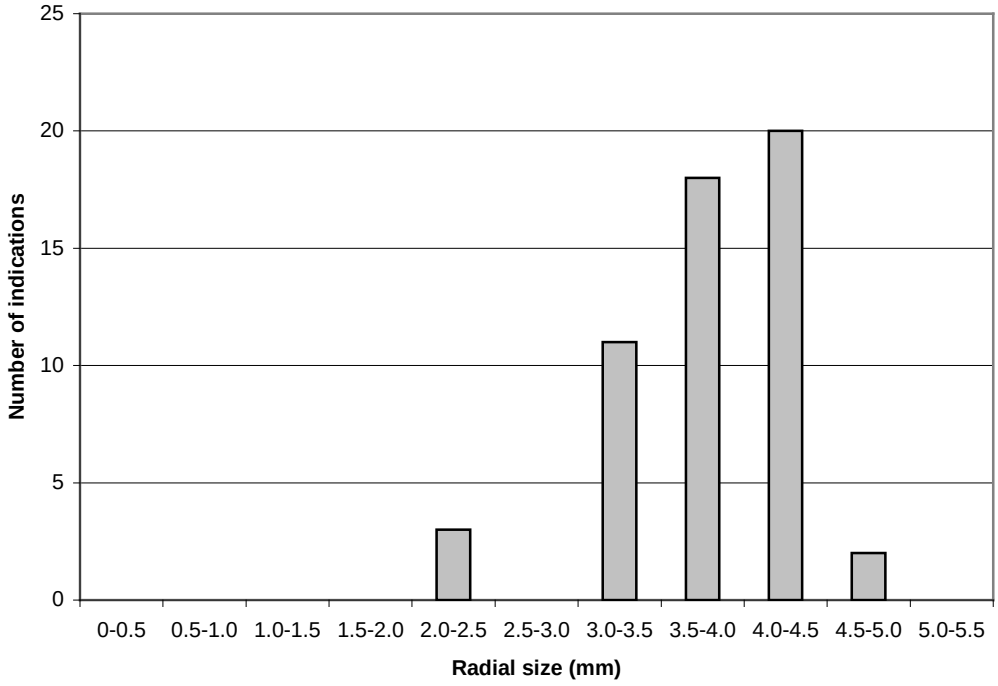

Figure 8-3. *Distribution of indicated defects in demonstration series performed by FSW.*

8.3 Examination of occurrence of defects not detected by NDT

The purpose of the examination was to determine the occurrence of the defects that are described in section 6.2, i.e. pores, oxide and metallic inclusions or other types of defects in the size range 0.1-3 mm.

8.3.1 Examination by destructive testing

The destructive tests were carried out using three methods:

1. Machining of weld specimens with area of 5.5 cm^2. Machining was done with 0.5 mm increments in the entire depth of the weld (50 mm), which meant 100 sections/specimen were studied under a magnifying glass. The purpose of these tests was to study defects larger than 0.5 mm.
2. Examination of polished macrospecimens (40x50 mm) under a microscope to determine the occurrence of defects larger than 0.1 mm.
3. Examination of single specimens in scanning electron microscope (SEM) plus refined microscopy for determination of occurrence of oxides.

Results

1. Examination in conjunction with machining was performed on 8 specimens from the demonstration series. No defects were found in these examinations /SKBdoc 1046524/.
2. As far as the examinations of macrospecimens are concerned, twelve specimens were studied. The distribution and type of indicated defects are presented below /SKBdoc 1040005/.
   - Five specimens exhibited clusters of copper oxide smaller than 300 µm.
   - Four specimens exhibited single pores or clustered porosities smaller than 0.5 mm.
3. The examinations for determination of oxide occurrence indicated strings of very small pores (1-10 µm) /SKBdoc 1175334/.

8.3.2 Examination by microfocus X-rays

20 test bars (20x20x80 mm) taken at random from all welds in the demonstration series were examined by microfocus X-ray and µ-CT at BAM /Müller C, et al, 2006/.

Results

The examinations with microfocus X-ray (see Figure 8-4) indicated no defects not indicated by the standard NDT.

8.4 Evaluation of post-demonstration series

In the first demonstration series, the maximum joint line hooking varied between 3.0 and 4.5 mm due to a longer probe than necessary. The post-demonstration series was therefore performed based on the later improved status of the welding procedure in fall 2006, using optimized probe geometry.

In this series, the NDT system did not indicate any defects besides 2.5 mm joint line hooking (JLH) at various locations. Macroscopic samples were collected at the maximum indicated JLH value for all 20 weld segments. Subsequent destructive testing showed that these maximum JLH values vary between 0.4 and 1.5 mm, with an average of 1.05 mm. The actual JLH values from the destructive tests were used for prediction of the future production quality of the welds, see section 9.2.2.

All welds were produced with the tool temperature inside the process window when welding at the joint line as can be seen inn Figure 8-4. It should be noted that no correlation between the tool temperature and the size of JLH have been found. Table 8-3 shows mean, minimum and maximum values as well as

standard deviations for the welding factors during the approximately 30 degrees of joint line welding for all weld segments in the post-demonstration series. Equivalent results for the welding responses, tool temperature and shoulder depth, are presented in Table 8-4. It should be noted that, like the demonstration series, the post-demonstration series could be carried out without any interruptions, which shows that process and system have high reliability and availability.

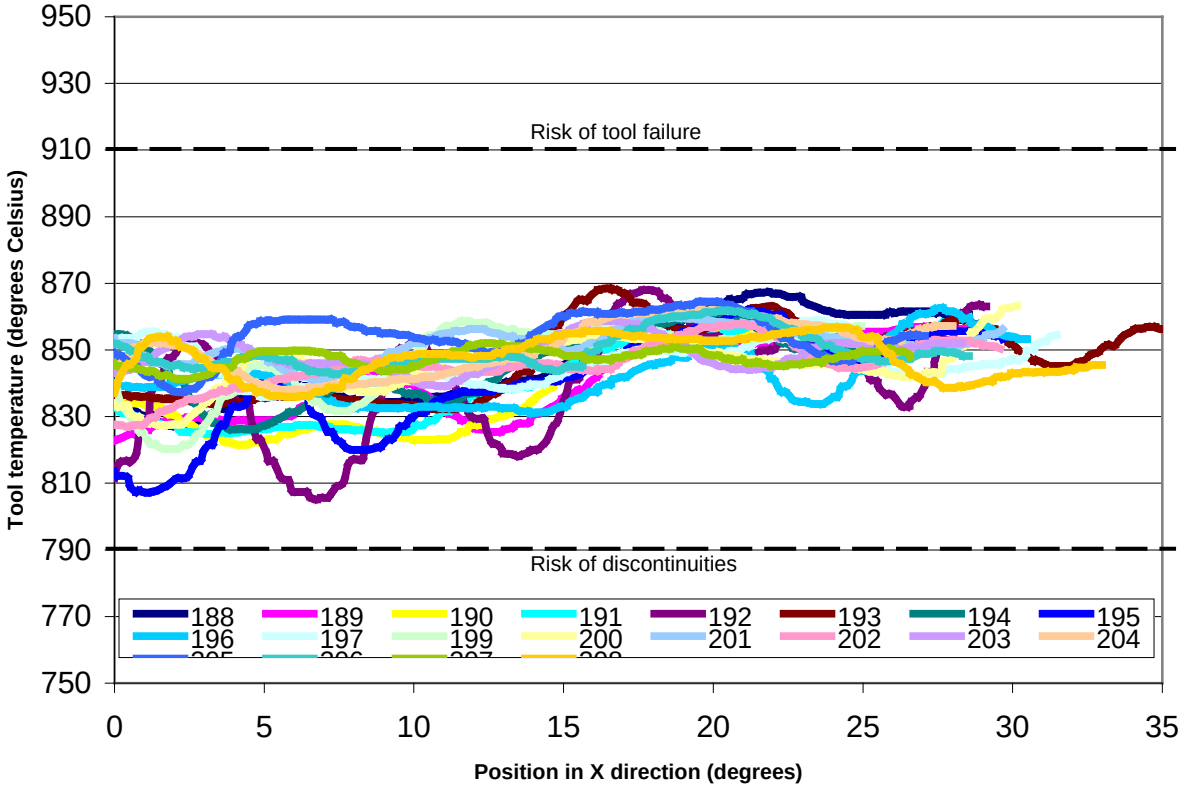

Figure 8-4. *Tool temperature during approximate 360 degrees of joint line welding with weld ID.*

Table 8-3. Welding factors in post-demonstration series.

	Spindle speed (SS)				Welding force (FZ)			
Weld ID	**Mean**	**Min.**	**Max.**	**St. dev.**	**Mean**	**Min.**	**Max.**	**St. dev.**
188	413	396	422	6,8	83,5	80,3	87,2	2,1
189	407	396	418	6,2	84,2	80,3	88,6	2,0
190	422	407	443	11,5	84,3	80,3	89,1	2,3
191	414	391	432	9,9	84,3	80,3	89,1	2,3
192	413	387	448	15,9	86,5	82,2	91,5	2,3
193	420	402	443	12,4	85,1	80,4	90,0	2,4
194	419	401	437	11,3	84,4	80,4	89,0	2,2
195	420	402	438	8,8	85,9	82,2	90,0	2,0
196	410	397	428	8,4	85,2	80,4	90,0	2,2
197	406	386	417	7,7	85,7	82,2	90,0	2,1
199	409	397	428	8,3	85,8	82,0	90,0	2,1
200	416	402	438	9,0	84,9	81,3	89,6	2,1
201	409	392	428	13,2	84,6	80,9	89,6	2,2
202	407	387	423	11,6	84,7	80,4	89,4	2,1
203	399	381	418	10,8	84,8	81,0	89,5	2,2
204	400	387	412	7,6	84,6	80,3	89,1	2,2
205	402	376	427	13,2	84,6	80,1	89,6	2,4
206	411	397	423	7,1	85,0	80,3	89,1	2,1
207	404	397	408	3,7	84,8	79,9	89,1	2,2
208	410	392	428	9,1	84,7	80,4	89,1	2,2
Mean	410	394	428	9.6	84.9	80.8	89.4	2.2

Table 8-4. Welding responses in post-demonstration series.

	Tool temperature (TT)				Shoulder depth	Maximum radial
Weld ID	**Mean**	**Min.**	**Max.**	**St. dev.**	**(PZ)**	**defect (mm)**
188	847	827	867	13,1	0,8	1,45
189	842	823	857	11,5	1,3	1,3
190	839	822	858	13,1	1,2	1,2
191	841	825	860	12,8	1,5	1,4
192	840	805	868	17,0	1,4	1,5
193	848	832	868	11,3	1,9	1,05
194	846	826	860	9,9	1,6	1,2
195	841	807	862	15,1	1,4	0,9
196	842	831	863	8,9	1,7	0,6
197	846	836	859	6,0	2,3	1,4
199	847	820	859	11,5	0,6	1,1
200	846	827	863	7,6	0,9	0,95
201	852	841	860	4,8	0,6	0,95
202	846	827	858	7,1	0,7	1,25
203	849	839	859	4,9	0,9	0,65
204	851	838	862	7,9	1,1	1,05
205	854	837	865	6,8	0,9	1,2
206	850	843	862	5,5	1,0	0,7
207	848	841	852	2,7	0,8	0,4
208	848	836	857	6,3	0,9	0,8
Mean	846	829	861	9.2	1.2	1.1

8.5 Mechanisms that cause formation of defects

Four types of defects were detected by non-destructive and destructive testing of the demonstration series.

A. Only one type of defect was detected by NDT in the lid welds in the demonstration series. This is the so-called joint line hooking (JLH) that occurs when the tip of the probe penetrates too deeply into the material and pulls the vertical joint between lid and tube against the tool shoulder, see Figure 6-1. JLH normally occurs in the overlap sequence, since the tool goes a little deeper there.

B. Pore strings formed when non-optimal welding variables were used. For example, when the welding variables were close to the limit for the tested process window (Table 4-8). Single pores were then detected at random in several welds.

C. Oxide occurrence was detected since the process takes place in the air and the heated joint surfaces react with the oxygen in the air.

D. Metal particles that can be traced to the tool were detected. These particles are detached from the tool probe due to the properties of the material at the high temperatures and forces that arise in the process.

8.6 Demonstration of preventive measures against defects

The four types of defects described in section 8.4 can be prevented by the following measures:

A. After the demonstration series, the development of the welding process was focused on eliminating or minimizing the JLH. This was shown in the post-demonstration series.

B. Welding within the process window.

C. The oxides only occur as tiny particles with an estimated size of 0.005 mm and maximum concentration of 25 ppm. Welding trials in argon gas has shown that the amount of oxide particles can be reduced.

D. Like the oxides, the metal particles occur as tiny particles with maximum concentration of 40 ppm. The currently used surface treated probe has reduce this value.

9 Prediction of future production quality

Future system performance for the encapsulation process is dependent on both the welding method and the non-destructive testing methods. Initially, an evaluation of the combined probability based on the estimated statistical distributions was therefore planned. However, the evaluation of the results from the demonstration trials with FSW did not show any future occurrence of defects larger than 7.7 mm, see below. Future system performance was therefore estimated directly from measurement data for the welding process and the NDT system was regarded as an extra, independent system for quality assurance.

The statistical evaluation of the first demonstration series was performed based on the programme of 4500 canister. In the evaluation of the post-demonstration series the analysis considers the programme of 6000 canisters. The analysis is also taking into account the welds for both the base and lid, giving a total amount of 12000 welds.

The statistical methods used in the evaluation, as well as experience from use in closely-related applications, were previously been discussed in a special method report /Müller and Öberg, 2004/. Results from this reliability study have also been reported in a scientific peer-reviewed journal /Cederqvist and Öberg, 2008/.

9.1 Statistical methods

The most common statistical models and methods are intended to characterize the occurrence of ordinary events, for example the population mean. These models do not work as well for assessing unusual events. Extreme value is another name for an unusual event, and the extreme value theory has been developed to handle such problems in different areas of technology, economics and environmental science. One area where extreme value models are needed is in the estimation of events that are so unusual that they have not yet occurred. Naturally it is possible to question the entire rationale behind such an extrapolation, but in many contexts a logical basis is needed to handle extreme events. The extreme value paradigm offers such a basis, and no credible alternatives have yet been presented.

The rationale behind the extreme value paradigm is similar to the central limit theorem, but now applied to maxima instead of sums. Suppose that X_1, X_2 … X_n is a sequence of independent random variables for an unknown distribution function F(x). Then the distribution of normalized maxima, M = max(X_1, X_2 ... X_n), for large values of n (n→∞) will converge towards one of three types of extreme value distributions: Gumbel, Fréchet or Weibull. These limiting distributions can then be used for statistical analysis of extreme values based on a finite number of samples.

The three extreme value distributions can be regarded as special cases and are summarized in the generalized extreme value (GEV) distribution:

$$G(z) = \exp\left\{-\left[1+\xi\left(\frac{z-\mu}{\sigma}\right)\right]_+^{-1/\xi}\right\}$$

where $\sigma > 0$, μ and ξ are real parameters, and $z_+ = \max(0,z)$.

The generalized extreme value distribution is suitable for modelling the distribution of maxima within defined intervals of time or space. Each interval is represented by a maximum. The estimated maximum distribution can then be extrapolated to the desired time, distance, etc. For the GEV distribution, if the shape parameter ξ is negative, the distribution has an upper finite limit.

9.2 Results

Two test series of FSW welds were evaluated. The first *demonstration series* consists of 20 welds, each run for a complete revolution (360˚) under production-like conditions. The second *post-demonstration series* also consists of 20 runs, but was performed with shorter (30˚) lid segment welds.

9.2.1 Results from the demonstration series

All 20 welds in the demonstration series were examined by Non-Destructive Testing (NDT) – phased array ultrasonic testing and digital radiography – according to the Canister Laboratory's procedures. No volumetric defects were detected by digital radiography, while ultrasonic testing indicated a total of 54 defects. Joint line hooking (JLH) was indicated in all welds with a radial extent in the range 2-5 mm.

A GEV distribution was fitted to NDT measurement data from the FSW process. The maximum defect (radial extent) in the weld served as a basis for the modelling, Table 9-1.

Table 9-1. Maximum defect size (radial extent) in FSW weld.

Weld ID	Maximum defect (mm)
22	3.0
23	4.5
24	3.5
25	3.5
26	3.5
27	3.5
28	4.0
29	4.0
30	4.0
31	4.0
32	3.5
33	4.0
34	4.0
35	4.5
36	4.0
37	3.5
38	4.0
39	3.5
40	3.5
41	4.0

The model parameters (standard errors within parentheses) were estimated using the maximum likelihood approach:

- $\mu = 3.673$ (0.09152)
- $\sigma = 0.3676$ (0.06508)
- $\xi = -0.2953$ (0.1597)

The results of fitting the GEV model are shown in Figure 9-1.

Figure 9-2 shows the expected maximum size of a defect as a function of the number of canisters fabricated. The right-hand end points of the lines in the graph correspond to the estimated maximum defect size in the welding of 4500 canisters.

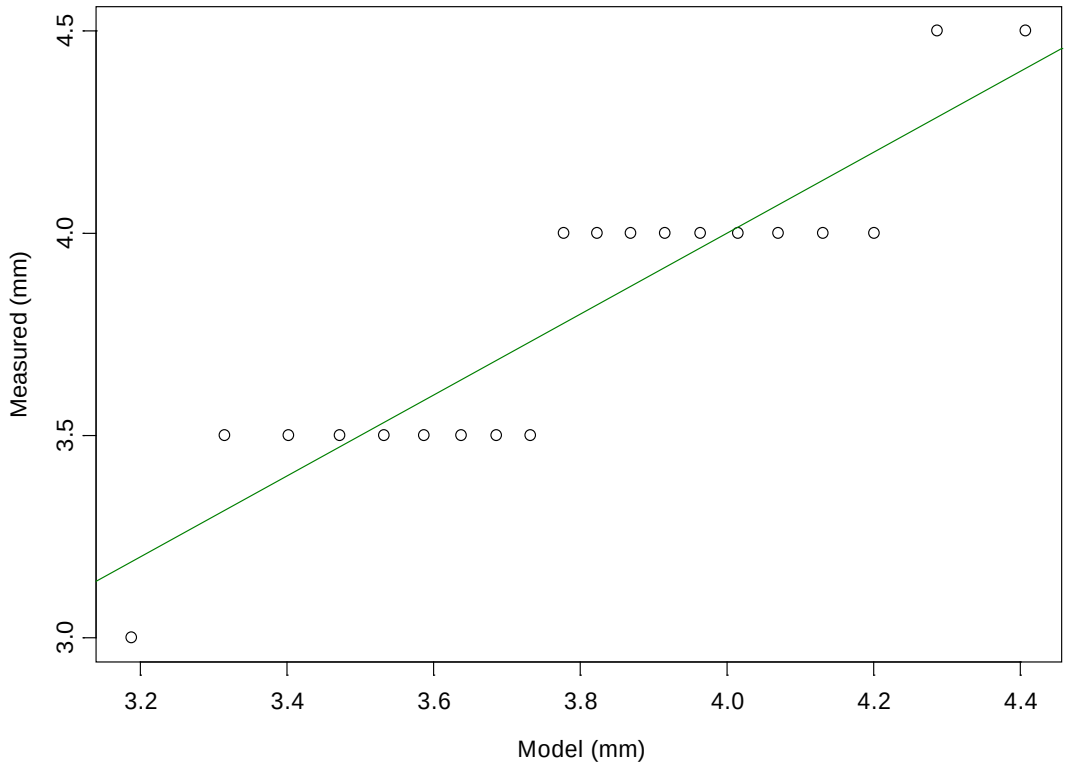

Figure 9-1. *GEV model fitted to NDT measurement data (ultrasound) for the FSW process.*

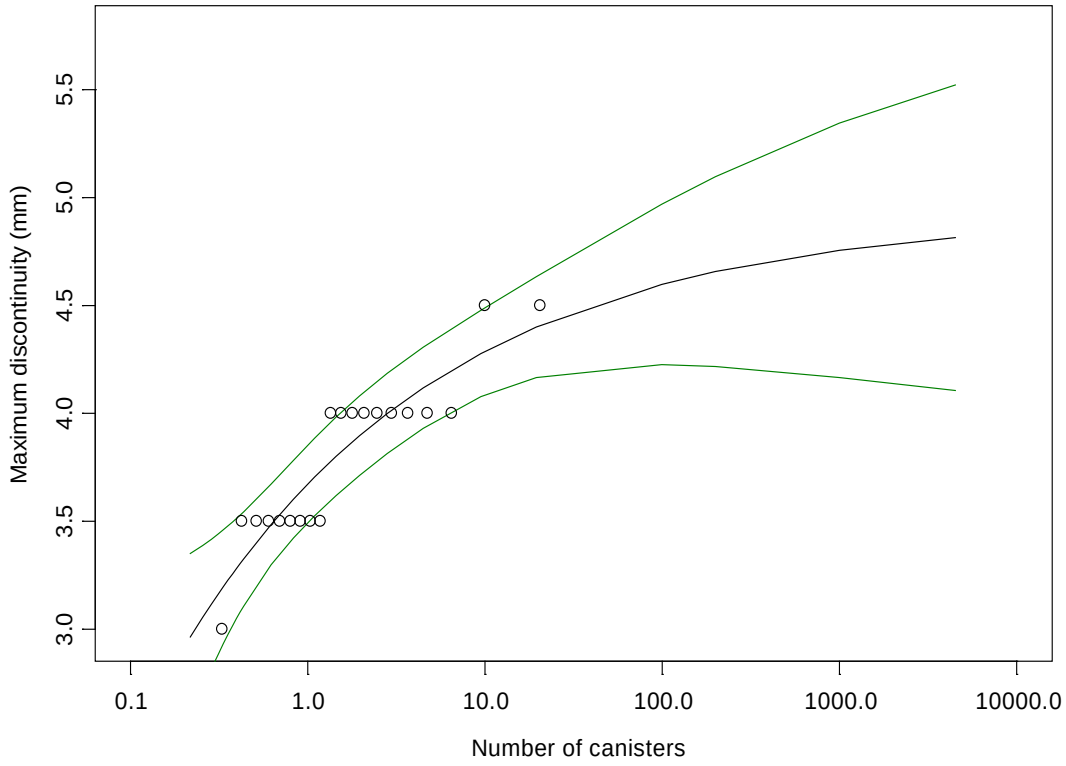

Figure 9-2. *Estimated maximum defect size, with confidence limits, in the production of different numbers of canisters.*

The confidence bands shown in Figure 9-2 can be estimated with greater certainty by using the profile likelihood method, which is described in a previous technical method report /Müller and Öberg, 2004/. The 95% confidence limits for the maximum defect in the fabrication of 4500 canisters then vary in the interval 4.5 to 7.7 mm.

The maximum estimated defect size in a production series of 4500 canisters has a radial extent of 4.8 mm, which is equivalent to a remaining thickness of 45.2 mm (50-4.8). The upper 95% confidence limit of 7.7 then corresponds to a minimum residual thickness of 42 mm.

The data reported in Table 9-1 has a resolution of 0.5 mm and can thus be regarded as discrete. An alternative GEV model was fitted with this constraint. This discrete GEV model has a similar, but lower asymptotic limit for the maximum size of a defect = $\mu - \sigma / \xi = 3.431 - (0.3364 / -0.2815) = 4.6$ mm. This difference between the continuous and discrete models is also obvious when comparing the probability density functions, Figure 9-3. The previously reported estimations, based on a continuous model, can therefore be regarded as conservative.

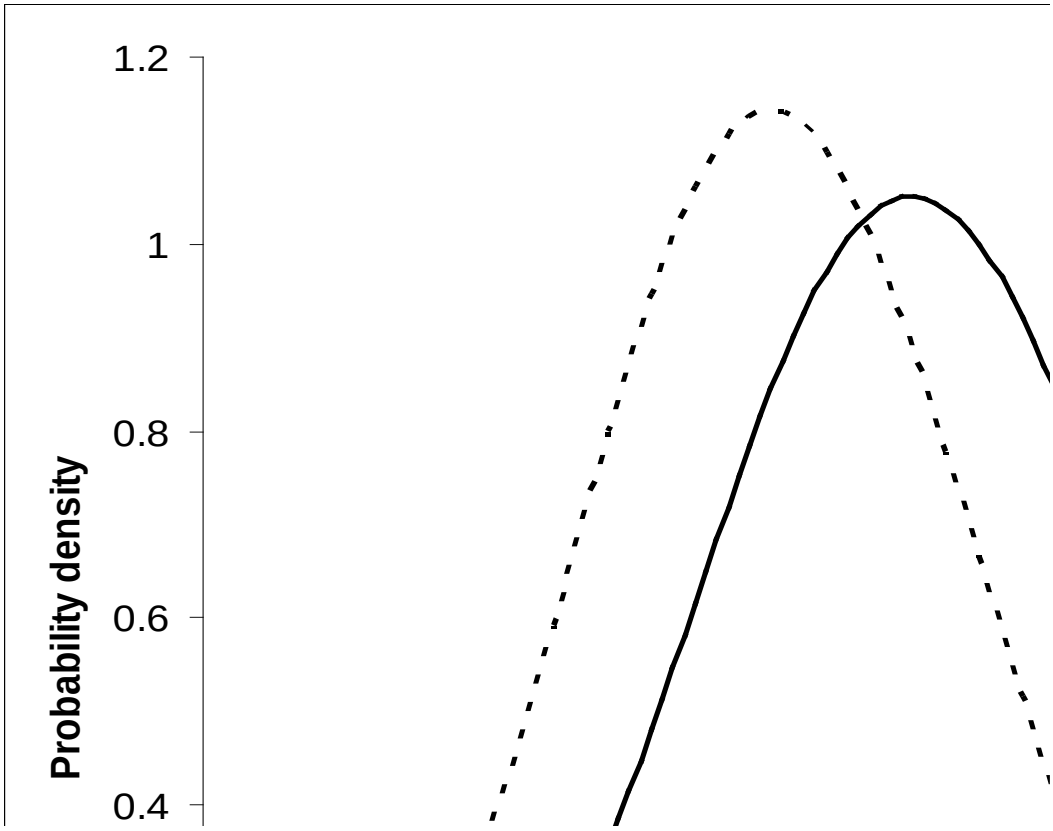

Figure 9-3. *The probability density functions for continuous and discrete GEV models fitted to NDT measurement data (ultrasound) for the FSW process.*

9.2.2 Results from the post-demonstration series

In the first demonstration series, the maximum joint line hooking varied between 3.0 and 4.5 mm due to a longer probe than necessary. A post-demonstration series has therefore been completed based on the current status of the FSW process, using a probe with optimized geometry. In this series, shorter weld segments were used that contains start above the joint line, down-travel, approximately 30˚ of joint line welding, overlap of the previous segment and park.

The NDT system indicated no defects except 2 and 2.5 mm joint line hooking (JLH) at various locations. Drill plugs were collected at the maximum JLH value for all 20 weld-segments. Subsequent destructive

testing showed that these maximum JLH values vary between 0.4 and 1.45 mm. The actual JLH values from the destructive tests were used for modelling the future production performance of lid welds, as before with a generalized extreme value (GEV) distribution, Table 9-2.

Table 9-2. Maximum JLH size in the weld, post-demonstration series.

Weld ID	Maximum defect size (mm)
188	1.45
189	1.3
190	1.2
191	1.4
192	1.5
193	1.05
194	1.2
195	0.9
196	0.6
197	1.4
199	1.1
200	0.95
201	0.95
202	1.25
203	0.65
204	1.05
205	1.2
206	0.7
207	0.4
208	0.8

The model parameters (standard errors within parentheses) were estimated using the maximum likelihood approach:

- $\mu = 0.9998$ (0.08359)
- $\sigma = 0.3377$ (0.07241)
- $\xi = -0.6329$ (0.2014)

The appearance of the GEV distribution is determined to a great extent by the shape parameter ξ. The current model also has a negative shape parameter and therefore an asymptotic limit for the maximum size of a defect $\mu - \sigma / \xi = 0.9998 – (0.3377 / – 0.6329) = 1.53$ mm.

The fitting of the GEV model is shown in Figure 9-4. The estimated maximum size of a defect as a function of the number of lid welds is shown in Figure 9-5.

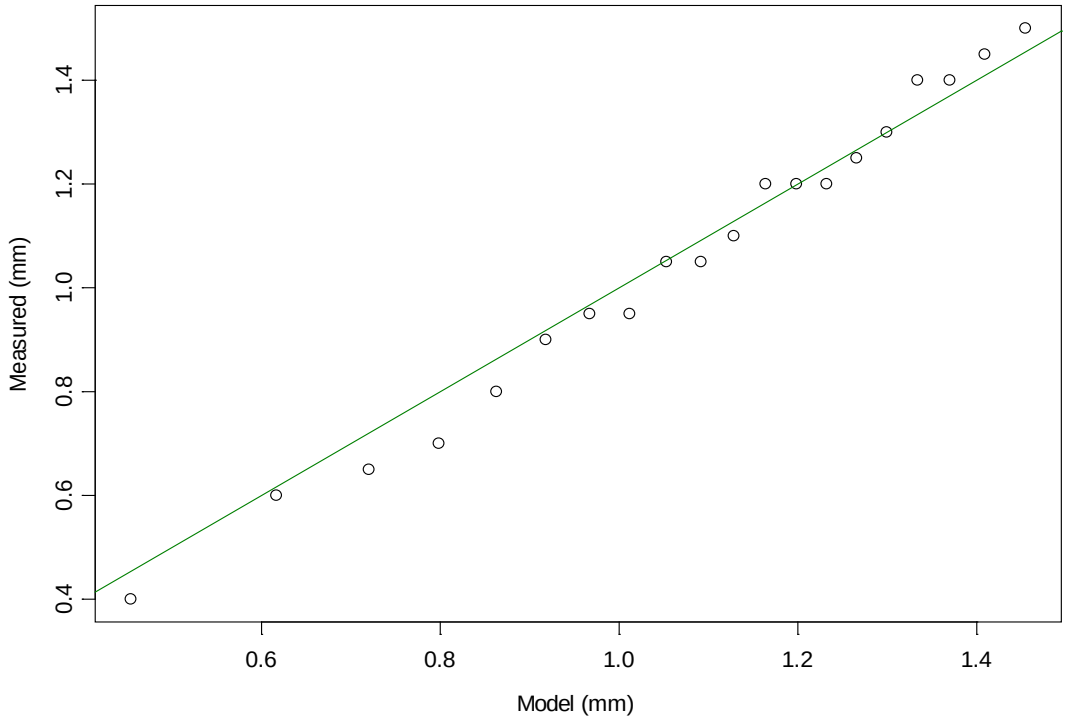

Figure 9-4: GEV model fitted to destructive measurement data for the FSW process.

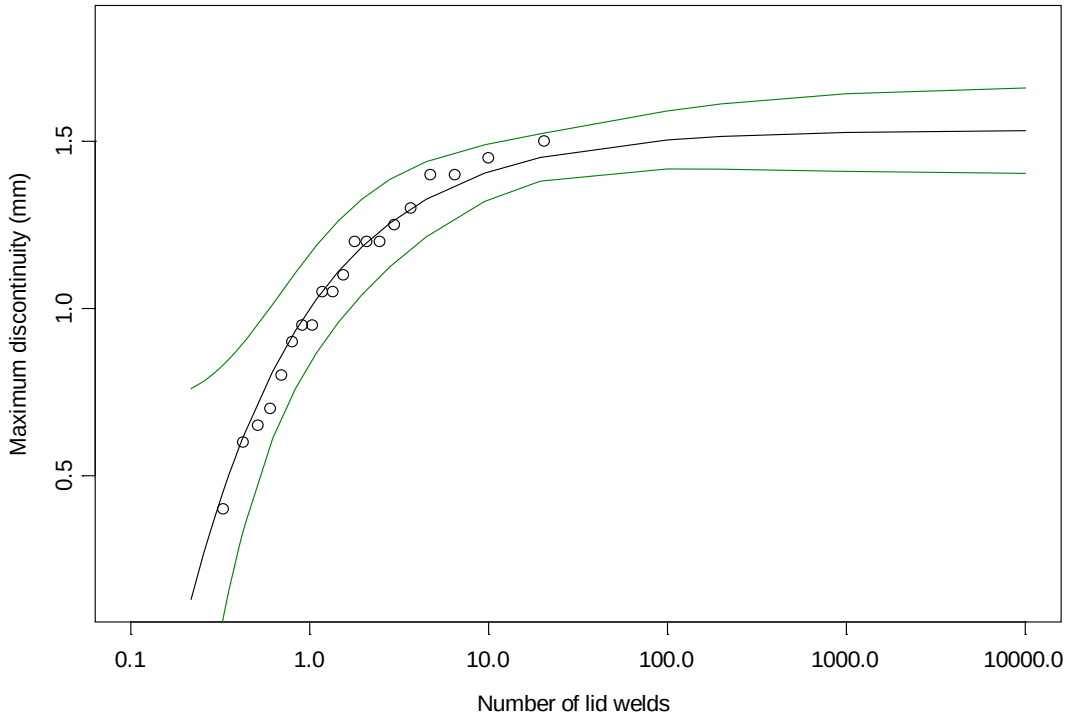

Figure 9-5: Estimated maximum defect size, with confidence limits, for 1–10 000 lid welds.

The confidence bands shown in Figure 9-5 can be estimated with greater certainty by using the profile likelihood method, which is described in a previous technical method report /Müller and Öberg, 2004/. The upper 95% confidence limits for the maximum defect in the lid welds are reported in Table 9-3.

Table 9-3. Upper 95% confidence limit estimated with the profile likelihood method

Number of 30˚ lid welds	Upper confidence limit (mm)
4 500	2.14
6 000	2.16
9 000	2.17
12 000	2.19

The parameters in the extreme value model were estimated from the maximum JLH defects detected in 20 lid welds. The best estimate of the maximum JLH defect after fabrication of 4 500–12 000 such welds is 1.53 mm, which is equal to the previously reported asymptotic limit. Additionally, the uncertainty in the parameter estimate is such that it is reasonably certain that the maximum size will not exceed 2.14–2.19 mm (95% confidence limit). The small variation in the estimated maximum JLH defect and the stable upper confidence limit is due to the excellent fit of the statistical model, as is apparent from Figure 9-4.

The 30˚ joint line welding encompasses 1/12 of a full rotation for the canister. Since defects were evenly spread, without clustering, it seems appropriate to evaluate the number of 30˚ lid welds multiplied by a factor of twelve, Figure 9-6 and Table 9-4.

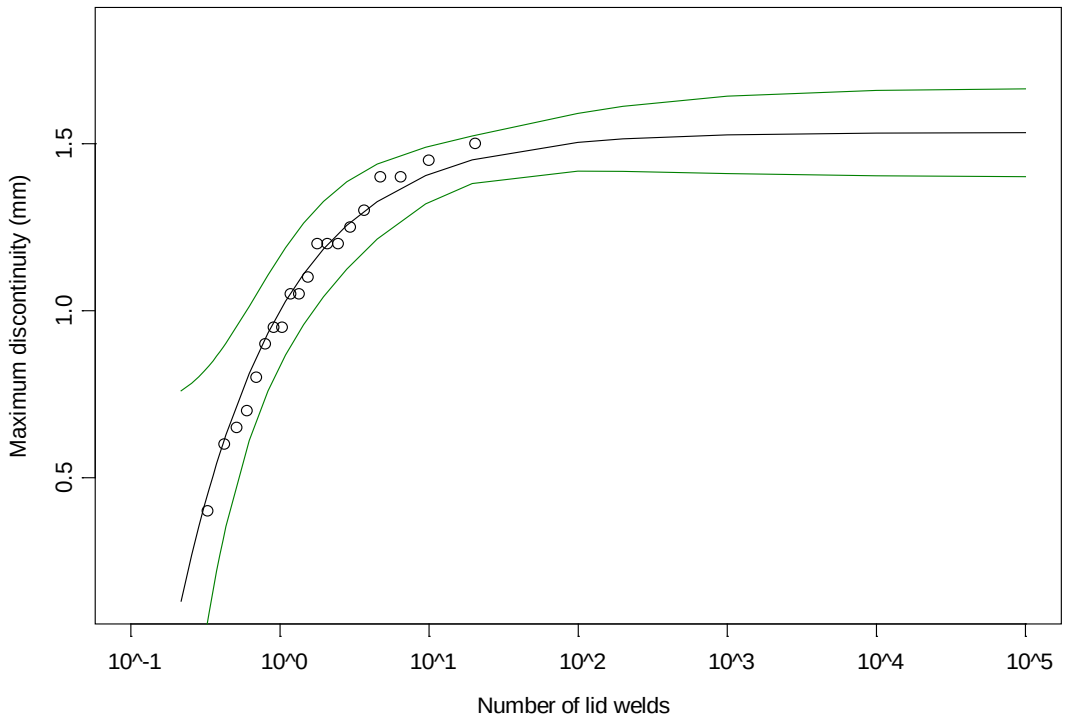

Figure 9-6: Estimated maximum defect size, with confidence limits, for 1–100 000 lid welds.

Table 9-4. Upper 95% confidence limit estimated with the profile likelihood method

Number of 30˚ lid welds	Corresponding number of canisters	Upper confidence limit (mm)
54 000	4 500	2.24
72 000	6 000	2.25
108 000	9 000	2.26
144 000	12 000	2.27

The best estimate of the maximum JLH defect after fabrication of 54 000–144 000 30° welds is as before equal to the asymptotic limit of 1.53 mm. Additionally, the uncertainty in the parameter estimate is such that it is reasonably certain that the maximum size will not exceed 2.24–2.27 mm (95% confidence limit). The excellent fit of the statistical model is obviously an important condition to support the chosen experimental strategy, with multiple test runs on each lid followed by extrapolation.

9.3 Prediction error and measurement uncertainty

The parameters in an extreme value model were estimated from the maximum defect size detected by ultrasound in the lid welds on 20 canisters in the demonstration series. The confidence limits express the uncertainty in the parameter estimates. The best estimate of the maximum defect after fabrication of 4500 canisters is thus 4.8 mm, but the uncertainty in the parameter estimate means that it is only possible to stipulate with certainty the that the maximum size will not exceed 7.7 mm (95% confidence limit).

Measurement uncertainties contribute to the uncertainty of the parameter estimate. A series of comparisons between ultrasonic testing and destructive testing indicate that the standard deviation is approximately 1 mm. This random part of the measurement error contributes to the parameter uncertainty and is included in its description. Beyond this there is also a systematic deviation that needs to be added to the model estimates. It is possible to use the mean of the residual values as a measure of the systematic deviation, but at least for joint line hooking the measurement error is systematically dependent on the defect size. A conservative estimation is therefore to add the maximum measured defect size that entails an underestimation to the previously stipulated confidence limit for maximum size, i.e. 7.7 + 2.1 = 9.8 mm. If both parameter uncertainty and systematic measurement error are taken into account, it is reasonable to assume a maximum defect size of 10 mm in the future production of welds under the same conditions as during the trials described here.

The expected maximum defect is dependent on the number of canisters fabricated, but when the upper confidence limit is estimated with the profile likelihood method, the differences are small. The maximum defect, including measurement error, can be estimated to be 7.8, 8.9 and 10.3 mm for a production series of 100, 1000 and 10000 canisters, respectively. Consequently, the minimum copper coverage within the entire planned fabrication interval should be estimated at 4 cm for a 5 cm thick canister.

An additional extreme value model was estimated from the maximum defect sizes detected by destructive testing of 20 short lid welds in a post-demonstration series, where a probe with optimized length was used. Using these data for the statistical modelling, the best estimate of the maximum JLH defect after fabrication of 54 000–144 000 30° welds, corresponding to both sealing and base welds for 6 000 canisters, is equal to 1.53 mm. Adding the uncertainty in the parameter estimate, the maximum size will not exceed 2.24–2.27 mm (95% confidence limit).

The previous estimate of the minimum copper coverage, within the planned fabrication interval of 6 000 canisters, thus seems conservative. There are, however, some additional uncertainties to consider for the post-demonstration series: possible defects not localised for destructive testing and the reduced length of the lid welds evaluated. It is therefore premature to change the previous estimate of 4 cm minimum copper coverage for a 5 cm thick canister, but these additional results should increase the confidence in this estimate.

10 Acceptance criteria

As is evident from Chapter 4, the welding process is robust and generates welds of very good quality over a wide process window. The reproducibility of the process is also very good, as shown by the demonstration series. The verification experiments (Chapter 4) show that it is possible to control the welding process by controlling the welding variables. By logging the variables it is possible to ensure afterwards that the process has been kept within the permissible process window.

10.1 Strategy

The objective in formulating the acceptance criteria for the Welding Section is to guarantee the predicted future production quality. This means that the criteria must include limits for the welding variables, but also guarantee a robustness against possible unidentified disturbances, which requires an independent NDT step.

The steps in the verification of the weld are shown in Figure 10-1 below.

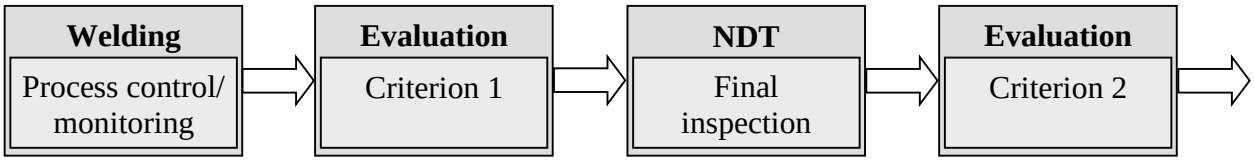

Figure 10-1. *Schematic diagram of weld verification against various criteria.*

10.2 Acceptance criteria

The weld's acceptance criteria consist of two parts that include both the welding process and the weld metal.

10.2.1 Acceptance criterion of the welding process

Criterion: The welding variables shall lie within the process window.

The smallest copper coverage on any canister in future production can then be estimated at 4 cm. The process window is defined in Table 4-8. Changes and improvements in the process and the welding system may require further studies of the process window. In conjunction with qualification of the welding process, a Welding Procedure Specification (WPS) is normally compiled. A WPS includes requirements on the tolerances of variables.

10.2.2 Acceptance criterion of the weld quality

Criterion: The extent of defects shall not reduce the corrosion barrier with more than ten millimetres.

This criterion includes limits for permissible indications in NDT and is based on the analyses in SR-Can /SKB, 2006b/. These analyses takes into account that all canisters welded under normal operation will have defects that maximum reduce the corrosion barrier by ten millimetres.

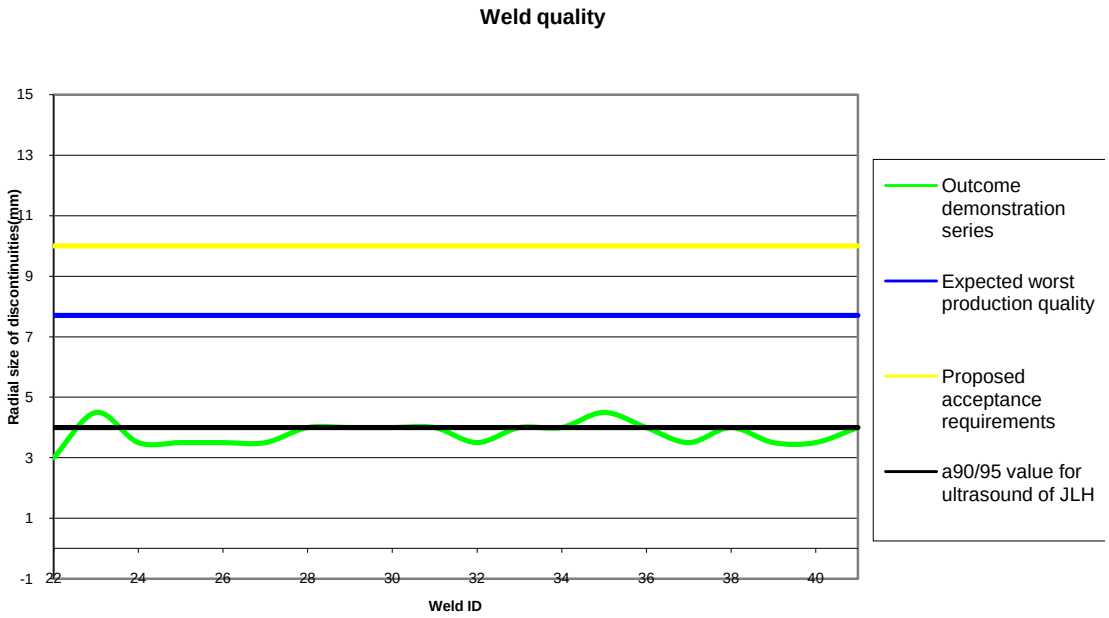

Figure 10-2. *Comparison between maximum measured defect sizes in the demonstration series, expected production quality, requirements according to the analyses in SR-Can, $a_{90/95}$ value for the ultrasonic inspection and proposed acceptance requirements.*

10.3 Application of the proposed acceptance criteria

If one of the criteria is not met, the sealed canister should be dealt with as a non-conformance. Examples of corrective measures for non-conformances are:

1. Re-welding: There is no reason why the canister cannot be re-welded by FSW. A weld that fails to meet one of the criteria can, after study and correction of the welding system, be re-welded. If the acceptance criteria are met after re-welding, the weld can be approved.
2. Rejection: Rejection is an option in the event of irreparable damage. For example, if the welding tool has broken and part of the probe is buried in the weld metal or a large geometric imperfection has arisen during welding.
3. NDT approval: In the event of a small deviation from criterion 1, the weld can be approved provided that criterion 2 is met with good margin.

Until further knowledge has been obtained; the second alternative, with rejection of the canister, will be treated as the reference corrective action.

10.4 Comments

NDT in future production will primarily be used to verify the process and ensure that the premises regarding clear relationships between production quality and welding variables that have been demonstrated in this study apply. This means that production statistics based on NDT and welding variables in the process should be continuously analyzed and used to control the processes. Use of NDT will enable any currently unidentified error mechanism that arises in the welding process to be detected.

Due to the fact that the handling safety of the canister only has been verified for one case, a 10 mm defect around the whole circumference is the acceptance criteria for the NDT limited. To be able to optimize these acceptance criteria, complementary calculations of the handling safety of the canister will be carried out. These calculations will most probably make it possible to increase the maximum radial size for isolated defects and the allowed remaining wall thickness.

11 Conclusions

Based on the completed investigation, the most important conclusions are:

- The welding process produces reproducible results with a predicted minimum copper coverage of 4 cm. This was further verified by the performed post-demonstration series.
- Control and logging of the welding variables can be used as a method to control the process.
- Non-destructive testing can be used to verify the weld quality with adequate reliability.
- The methodology for statistical experimental planning has been implemented with good results and SKB plans to use this methodology for reliability studies of other Sections in the production system.

12 Future line of action

The development of the FSW process and the associated NDT process has gone very quickly. This report has shown that the processes that were developed up to the end of 2007 and that have been evaluated have very good potential to be used in a future production system within the Welding Section. The continued development work with the reliability of the process will be focused on further optimizing the process and verifying the results that have emerged in this investigation.

Further investigations concerning the connection between the welding variables and results from NDT will be conducted to further verify the conclusions in this report. Changes and improvements of processes and systems for welding will require further investigations of the process window. In conjunction with qualification of the welding process, a final version of the WPS (Welding Procedure Specification) will be prepared. The WPS includes requirements on tolerances, i.e. process windows for welding variables.

12.1 Process FSW

Further development of the FSW process will be pursued according to the main lines presented in Table 12-1.

Table 12-1. Overall plan of FSW actions.

Activity	Contents
Automation of process.	The adaptive control of the process is currently manual. The software will be developed so that this can be done automatically to minimize the human factor. This will also enable the process to be regulated more quickly and precisely.
Optimization of welding process.	When the automated software is fully developed, the process should be optimized towards high stability and repeatability within as wide a process window as possible. The development work to increase the upper temperature limit of the process window and thereby also the safety factor will be pursued by testing new probe materials and surface treatment.
Evaluation of the composition and mechanical properties of the weld material	When the process is automated and optimized, further analyses of the weld material will be performed. These analyses will be done to verify that the material composition and properties fulfil the specifications in the reference design.
Acceptance criteria.	As input to the final acceptance criteria will further investigations of the formation of defects, be studied. Furthermore, development of the process window will enable acceptance criteria to be established for the welding process.

12.2 Process NDT

Further development of the NDT process will be pursued according to the main lines presented in Table 12-2. More detailed plans are presented in /SKBdoc 1179633/.

Table 12-2. Overall plan of NDT actions.

Activity	Contents
Optimization of NDT process.	The NDT process will be optimized by combining practical experiments with modelling of sound fields and their interaction with different types of defects. The goal is to obtain an optimized NDT process.
Study of important variables.	Carry out a statistical study of which variables influence the NDT. The study is planned to be conducted according to principles similar to the study of the welding process.
Evaluation of material properties	Study what effects the properties of the lid material in terms of structure and defects have on the NDT.
Acceptance criteria	Formulate and adopt acceptance criteria based on supplementary knowledge from material examinations and the optimized NDT process.

13 References

SKB's (Svensk Kärnbränslehantering AB) publications can be found at www.skb.se/publications. References to SKB's unpublished documents are listed separately at the end of the reference list. Unpublished documents will be submitted upon request to document@skb.se

Box G E P, Draper N R, 1987. Empirical model-building and response surfaces. Wiley, New York, USA

Box G E P, Hunter W G, Hunter J S, 1978. Statistics for experimenters: An introduction to design, data analysis, and model building. Wiley, New York, USA

Cederqvist, 2006. Friktionssvetsning av kopparkapslar rapport 1, SKB Rapport R-05-73, Svensk Kärnbränslehantering AB

Cederqvist L, Öberg T, 2008. Reliability study of friction stir welded copper canisters containing Sweden's nuclear waste. Reliability Engineering & System Safety 93, pp 1491-1499

Efron B, Tibshirani R, 1993. An introduction to the bootstrap. Monographs on statistics and applied probability. Chapman & Hall/CRC,xvi, New York, USA

Gubner R, Andersson U, 2007. Corrosion resistance of copper canister weld material, SKB Report TR-07-07, Svensk Kärnbränslehantering AB

Müller C, Öberg T, 2004. Strategy for verification and demonstration of the sealing process for canisters for spent fuel, SKB Report R-04-56, Svensk Kärnbränslehantering AB

Müller C, Elagin M, Scharmach M, Bellon C, Jaenisch G-R, Bär S, Redmer B, Goebbels J, Ewert U, Zscherpel U, Boehm R, Brekow G, Erhard A, Heckel T, Tessaro U, Tscharntke D, Ronneteg U, 2006. Project NDT Reliability, final report, SKB Report R-06-08, Svensk Kärnbränslehantering AB

Ronneteg U, Moberg B, 2003. Inkapslingsteknik, Lägesrapport 2002, Oförstörande provning, SKB Report R-03-31, Svensk Kärnbränslehantering AB

Ronneteg U, Cederqvist L, Rydén H, Öberg T, Müller C, 2006. Reliability in sealing of canister for spent nuclear fuel, SKB Rapport R-06-26, Svensk Kärnbränslehantering AB

SIS, 2000. Non-destrutive testing – Ultrasonic examination – Part 5: Characterization ans sizing of discontinuities SS-EN 583-5, Swedish Standards Institute.

SIS, 2002. Welding and allied processes – Classification of geometric imperfections in metallic materials – Part 2: Welding with pressure SS-EN ISO 6520-2:2001, Swedish Standards Institute.

SKB, 2003. Planning report for the safety assessment SR-Can, SKB Report TR-03-08, Svensk Kärnbränslehantering AB

SKB, 2004. Programme for research, development and demonstration of methods for the management and disposal of nuclear waste, including social science research, Svensk Kärnbränslehantering AB, SKB Report TR-04-21, Svensk Kärnbränslehantering AB

SKB, 2006a. Kapsel för använt kärnbränsle – Svetsning vid tillverkning och förslutning, SKB Rapport R-06-04, Svensk Kärnbränslehantering AB

SKB, 2006b. Long-term safety for KBS-3 repositories at Forsmark and Laxemar – a first evaluation. Main Report of the SR-Can project, SKB Report TR-06-09, Svensk Kärnbränslehantering AB

US Department of defense, 1999. Non-destructive evaluation system. Reliability assessment, Handbook. MIL-HDBK-1823.

Unpublished documents

SKBdoc id,	version	Title	Issuer, year
1040005 ver	2.0	Dokumentation och uppmätning av skarvens utseende i FSW-prover, PRO05-0487 Framtagen av Bodycote CSM AB	SKB, 2005
1046524 ver	1.0	Förstörande prov ur demonstrationsserie FSW	SKB, 2005
1077122 ver	1.0	Strålskärmsberäkningar för kopparkapslar innehållande BWR, MOX och PWR bränsleelement, 07-0014R rev 0 Framtagen av ALARA Engineering	SKB, 2007
1175162 ver	4.0	Svetsning vid tillverkning och förslutning	SKB, 2008
1175235 ver	3.0	NDT Reliability	SKB, 2006
1175334 ver	1.0	Microstructure of friction stir welded copper joints Framtagen av Posiva R&D Report	SKB, 2006
1179633 ver	3.0	Oförstörande provning av kapselkomponenter och svetsar	SKB, 2008

14 Abbreviations

NDT	Non-destructive Testing
POD	Probability of Detection
ROC	Receiver Operating Characteristic
UT	Ultrasonic Testing
RT	Radiographic Testing
FSW	Friction stir welding
BAM	Bundesanstalt für Materialforschung- und Prüfung
IC	Intrinsic Capability
HF	Human factors
AP	Application parameters
μ-CT	Micro-focus Computed Tomography
HECT	High-energy Computed Tomography
MTO	Man Technology Organization